DESIGN FOR MANUFACTURABILITY OF A HIGH-PERFORMANCE INDUCTION MOTOR ROTOR

by

Christopher P. Brown

B.S. Aeronautical Engineering
Rensselaer Polytechnic Institute, 1994

B.A. Physics
Reed College, 1994

SUBMITTED TO THE DEPARTMENT OF MECHANICAL ENGINEERING
IN PARTIAL FULFILLMENT OF THE REQUIREMENTS FOR THE DEGREE OF

MASTER OF SCIENCE
at the
MASSACHUSETTS INSTITUTE OF TECHNOLOGY

JUNE 1996

Signature of Author: ....
Department of Mechanical Engineering
May 10, 1996

Certified by: ....
Jung-Hoon Chun
Esther and Harold E. Edgerton Associate
Professor of Mechanical Engineering
Thesis Supervisor

Accepted by: ....
Ain A. Sonin
Chairman, Department Committee on Graduate Students

Design for Manufacturability of a High-Performance Induction Motor Rotor

by

Christopher P. Brown

Submitted to the Department of

Mechanical Engineering on May 10, 1996

in Partial Fulfillment of the Requirements for the Degree of

Master of Science

ABSTRACT

A study is conducted on the state-of-the-art manufacturing practices of conventional industrial and research-and-development (R&D) firms manufacturing electric induction motors. It is found that current industrial processes cannot produce high-performance motors, and that current R&D processes are too costly. A new manufacturing process for fabricating the rotors of squirrel cage induction motors is developed. The new process addresses the issues raised by the study by delivering high performance at a reduced cost.

The induction rotor manufacturing process presented involves using net shape processes to manufacture the parts which are manually assembled and subsequently joined. A squirrel cage of extruded chromium copper bars and end rings is used. Investment casting is used to fabricate a core of high-strength Aermet. It is shown that it is necessary to open the slots of the magnetic core of the motor in order to make effective use of investment casting and to ease assembly. The effect on motor performance of changing materials and opening slots is analyzed. The squirrel cage, impellers and shaft can be manually assembled to the core. The assembly is then joined using a diffusion bonding process. The feasibility of a Cr-Cu/Aermet diffusion bond is experimentally verified.

A systematic method of designing and optimizing a manufacturing process is presented. It is based on the experience of designing the process for the rotor.

Thesis Supervisor: Jung-Hoon Chun
Title: Esther and Harold E. Edgerton Associate
      Professor of Mechanical Engineering

Table of Contents

List of Figures

List of Tables:

Chapter 1

INTRODUCTION

1.1 Purpose

When engineers design a product, they are generally faced with an array of manufacturing process options by which to fabricate it. Net-shape processes such as casting, forging, and powder metallurgy offer reasonable material properties and dimensional accuracy at affordable cost and high volume. Subtractive (material-removing) processes such as the various types of machining offer excellent and controllable part quality but at a higher cost. Still other processes can form special classes of materials (such as sheet metals or composites) at great advantage. There are hundreds of fabrication technologies, each of which has advantages and drawbacks in terms of the geometric capabilities and the material properties of the finished product.

Often, the best process choice for one part in an assembly is not the best choice for another. The processes can also interact: using a given process to make one part may introduce geometrical options which constrain or expand the manufacturing choices for another part. Optimal joining of parts becomes an issue when an assembly contains parts which do not move relative to one another while the device is in operation. In general, an engineer has no systematic method by which to create a manufacturing process for a part or an assembly of parts which is optimized in terms of part quality (e.g., materials properties and geometry) and cost.

The problem to be solved is: given a part, or an assembly of parts, determine the most cost-effective means of manufacturing it while maintaining a high standard of quality. A systematic method of inventing an optimized manufacturing sequence for a given assembly will be presented in abstract form in Chapter Five. The method will be developed in the context of a specific example of industrial significance: the manufacture of high power-density induction motors.

Sections 1.2 and 1.3 will explain the industrial uses and the functional principles of the high power-density electric induction motor to be fabricated. The manufacturing analysis will be focused on the rotor of the machine. Chapter Two will explain the shortcomings of current industrial manufacturing practice at making high power-density electric motors. It will also present the method currently used by SatCon Technology Corporation (SatCon) to fabricate its high power-density induction motors, in which some material choices have been made to enhance performance. While SatCon has solved some of the problems endemic in current industrial practice, the cost of their induction motors is still unacceptably high. Chapter Three will present the proposed manufacturing process and explain how it was designed. Chapter Four will present a cost estimate of the proposed production sequence and compare it to existing processes to demonstrate its cost effectiveness.

1.2 The Significance of High-Speed, High Power-Density Induction Motors

Most technologies which use rotating machinery can derive a performance benefit from higher rotational speeds. Turbomachinery, for instance, becomes more efficient with increasing rotational speeds (up to the onset of supersonic velocities) due to thinning boundary

layers at higher flow rates. As another example, machining efficiency increases with spindle speed due to lower cutting forces. The efficiency and power-density of electric motors increases with speed due to the lower torque required to generate a given power. Lower torque requires a smaller-radius, and hence lighter, machine.

Thus, electric machines are not only themselves more efficient at high speeds, but machinery operated by electric motors/generators (e.g., HVAC, compressors, gas turbine power generators, and machine-tool spindles) are more efficient as well. High-speed (and hence high power-density) electric machines are the enabling technology for the next generation of high speed machinery of all sorts.

High speed electric machines are used to reduce the size and weight and at the same time increase the efficiency of various sorts of drive systems. Currently, electric drives are often gear- or belt-connected to the machinery which they operate. Gears introduce losses, involve higher maintenance efforts, require extra sub-systems (e.g., an oil lubrication system or a water cooling system) and generally reduce efficiencies. Recent advances in power electronics make it possible to improve motor control and realize adjustable-speed drives, eliminating the need for intermediate gears. Power electronics essentially acts as an electronic gear box [1]. The design of high and variable speed drives, however, requires a fresh look at the design and manufacturing processes used to fabricate electric motors.

SatCon, the company which supported this research, has developed and constructed several prototype high speed induction machines for electric vehicle, aircraft APU (auxiliary power unit) and HVAC compressor applications. The traction motor shown in Figure 1.1, for instance, exhibits a power density of 3.65 kg/kW at a speed of 24,000 rpm and an output

power of 560 kW. Other SatCon motors have power to weight ratios of 3.5-4 kg/kW at speeds ranging from 60,000 to 100,000 rpm [2]. In contrast, a conventional 373 kW motor has a power density of around 7.3 kg/kW running at an operating speed of 3600 rpm [3], making it twice the weight of a SatCon motor for a given power output.

While the performance of these motors has been excellent, their utility is limited due to high manufacturing costs. The reasons for these high costs will be explored in Chapter Two, in which conventional industrial practice will be contrasted with the requirements placed on the materials and design by these unusually high power densities.
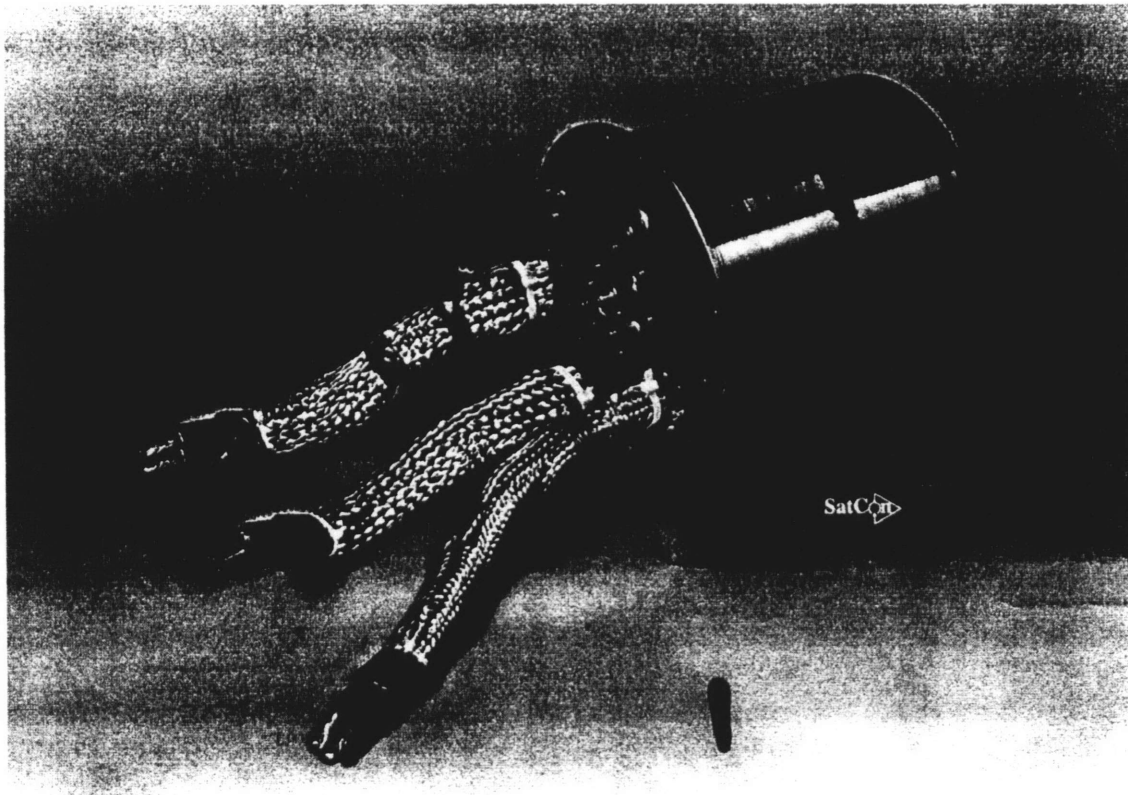
Fig. 1.1. The SatCon traction motor built for the Chrysler Corporation

Based on the experience of SatCon in assembling these motors, the most expensive parts of the assembly have been identified. The cost drivers are the rotor assembly and the stator stack. This thesis will focus on the design for manufacture of the rotor assembly.

1.3 Induction Motors: Operating Principles and Mathematical Modeling

Clearly, the first step in devising a manufacturing process is to understand the operating principles of the machine to be manufactured. Manufacturing engineers should also have access to design principles and software that allow them to evaluate the impact of design modifications on the performance of the machine. This section contains a brief description of the operating principles of induction motors and a description of the design software used to evaluate modifications. This section illustrates how induction machines work, and puts into context the seminal geometric and materials features of the motor.

1.3.1 Induction Motor Operating Principles

Figure 1.2 shows a typical induction motor. It is primarily composed of a rotor and a stator. By applying three sinusoidal currents 120° out of phase to the three phase windings of the stator, a radially oriented rotating magnetic field is generated which induces currents in the

bars of the rotor. The currents on the rotor and the stator interact to produce torque on the rotor.
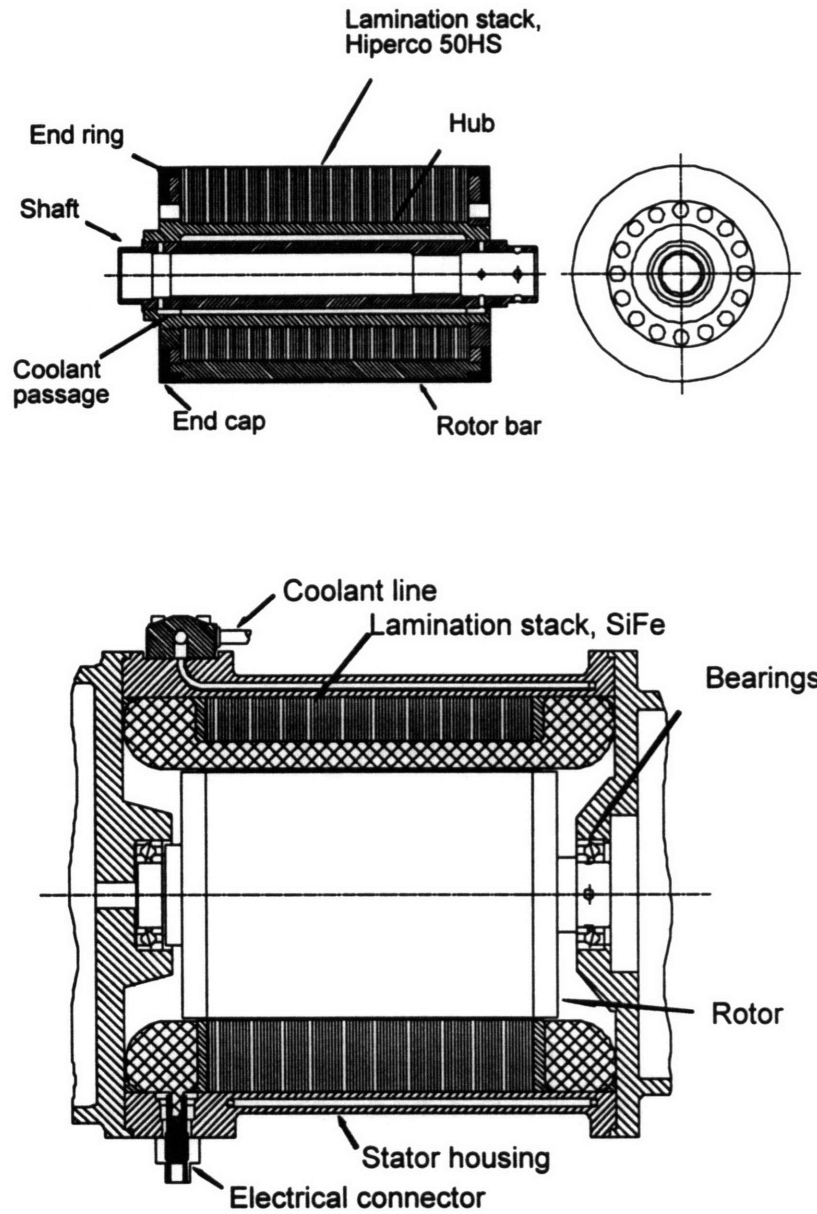
Figure 1.2. *Schematic of a typical induction motor illustrating the rotor assembly (above) and the rotor and stator (below)*

The process can be illustrated more clearly in the following manner. The magnetic field

of a current loop (or several current loops) wound around a piece of ferromagnetic material is

shown in Figure 1.3. In the loop, X indicates current flow into the page and a dot represents

current flow out of the page. This configuration is that of a solenoid. The field is that of a

magnetic dipole. It points along the direction of the axis of the loop, in the interior of the loop

in accordance with the right-hand rule (e.g., if one points one's right thumb in the direction of

the current, the fingers curl in the direction of the magnetic field).
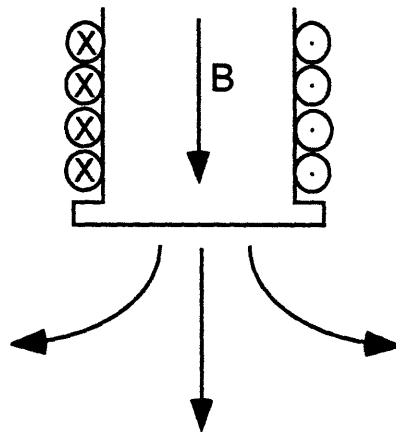
Figure 1.3. The magnetic field of a number of current-turns around a ferromagnetic material

The purpose of the ferromagnetic material is to increase the intensity of the magnetic

field. The magnitude of the magnetic field (per unit length) in the material is given by:

$$B=\mu NI \qquad (1.1)$$

where μ is the permeability of the material, N is the number of turns of wire and I is the current in the wire. The permeability of air (referred to as μ_o) is on the order of 10^{-7} N/A^2 whereas the permeability of a ferromagnetic iron alloy can be more than this by a factor of 10^4 or more [4]. This leads to a tremendous increase in flux density for an applied current which, it will be seen, increases the possible torque immensely.
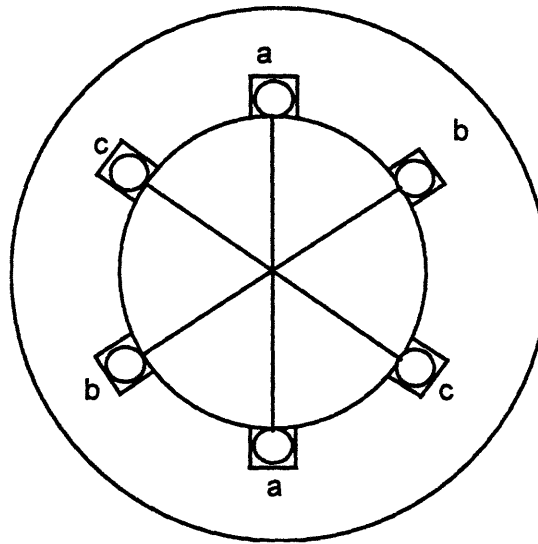
Figure 1.4. Conceptual picture of the stator illustrating the three phases a, b, and c

Suppose now that there are several current loops arranged in slots around a cylinder, as shown in Figure 1.4. The loops will create essentially radially oriented magnetic fields (neglecting fringing fields). Now suppose that each of the three loops is connected to a source of sinusoidally varying current and that the current in each loop is 120° out of phase with the

other two. Then, as a function of time, the magnetic field in the interior of the cylinder will

rotate as shown in Figure 1.5.
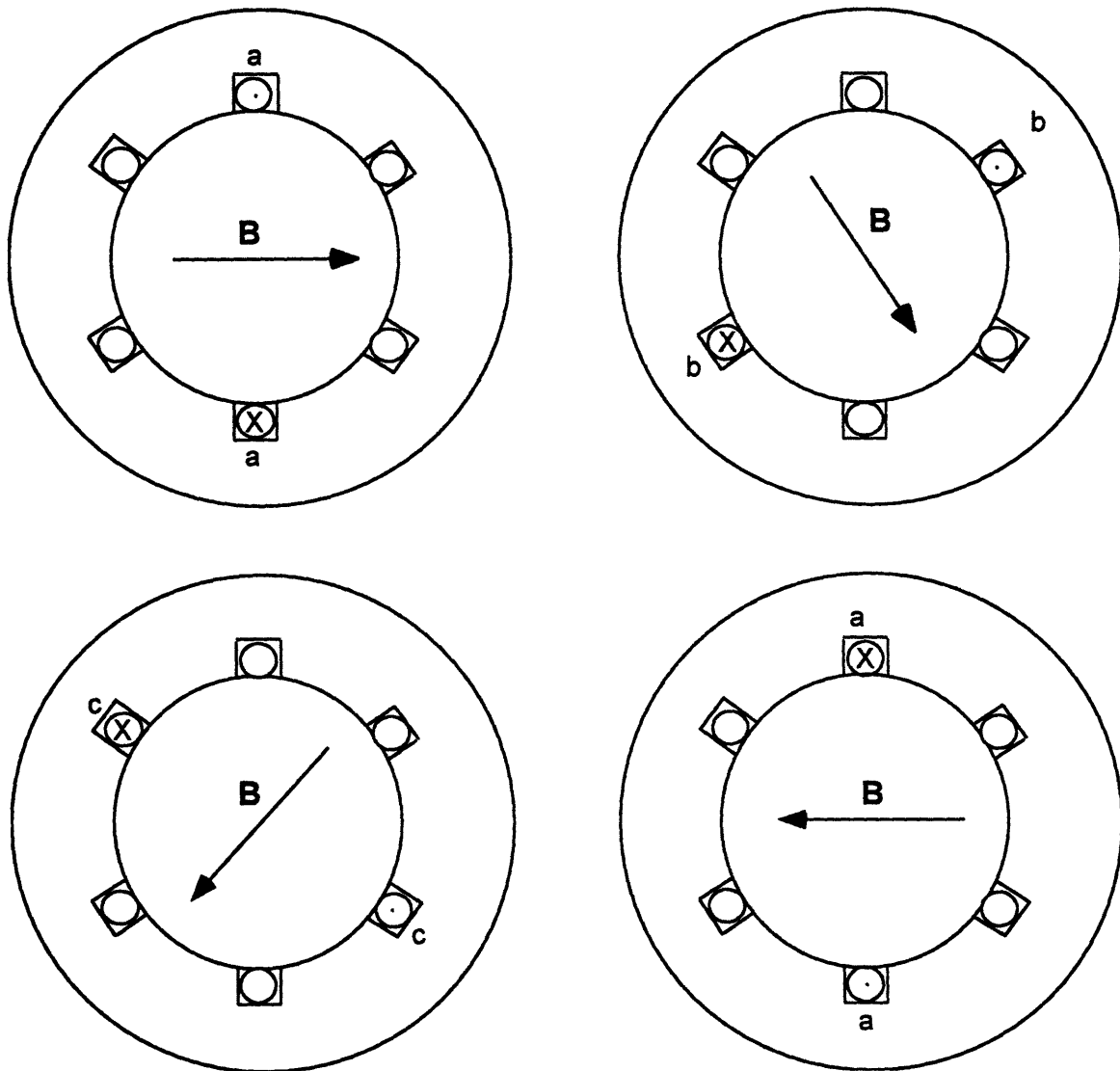
Figure 1.5. Illustration of how the three phases create a radially oriented rotating magnetic field

15

As the current in each loop reaches a maximum, the dominant field points in the direction

shown. Thus, for the simple stator shown, **B** makes a full rotation at the same frequency as

that applied to the phases. If there were more "poles", i.e., if each phase were routed to more

than one loop, the field would rotate more slowly.

It is now time to insert the induction motor's rotor into the hollow cylinder with its

rotating magnetic field. The time varying nature of the magnetic field will induce currents in

the bars of the rotor (the "squirrel cage") due to their mutual inductance. This can be seen

from Faraday's law:

$$\nabla \times E = -\frac{\partial B}{\partial t} \qquad (1.2)$$

This shows how a time-varying magnetic field induces a perpendicular electric field. The

electric field produces an axial voltage across the conducting bars of the squirrel cage. Since

the axial bars of the cage are shorted to one another by the end rings, current flows through

them. The rotor currents will produce torque according to the Lorentz force law for the force

on a current-carrying conductor in a magnetic field:

$$F = J \times B \qquad (1.3)$$

Equation (1.3) says that the force on a current carrying conductor is perpendicular to **J** and **B**.

Since **J** is axial and **B** is radial, **F** is circumferential, producing torque.
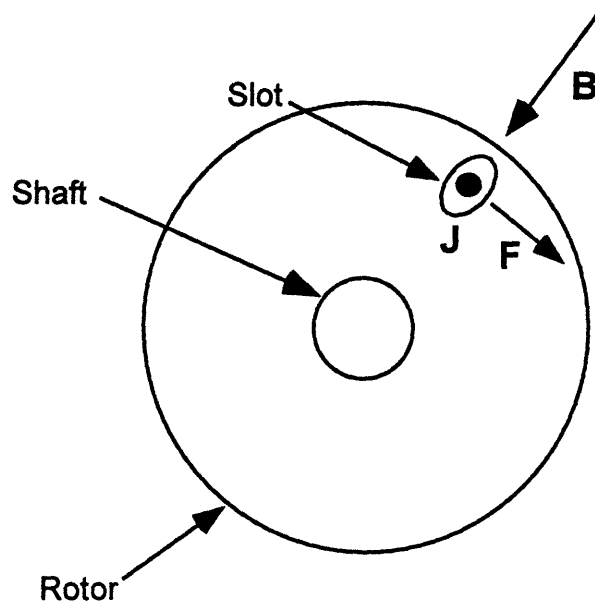
Figure 1.6: Induction rotor schematic showing the electromagnetic interaction of one slot

This process is simplified in Figure 1.6 with an axial view of the rotor: one slot is shown, although normally there would be from 15 to 30. The time-varying radial magnetic field induces an axial voltage in the conductors immersed in it, including the ferromagnetic core of the rotor. Since the core material is generally not as good a conductor as the bars (the bars are usually made of aluminum or copper while the core must be made of some ferromagnetic alloy), currents induced in the core generate more losses than torque and are generally considered undesirable. That is why most induction rotor magnetic cores are composed of stacks of strips of sheet metal known as laminations. The thin laminations break up the axial conducting path in the core, effectively confining rotor currents to the squirrel cage [5].

Thus, the torque produced by the machine will be the force on the rotor over the surface area times the moment arm (i.e., the rotor radius) [6]:

$$T=2\pi R^2 l<\tau> \tag{1.4}$$

17

where T is the torque developed, R is the rotor radius, l is the rotor length and $<\tau>$ is the average electromagnetic shear. From the Lorentz force law (Equation 1.3), the electromagnetic shear is:

$$\tau \propto B_r K_z \qquad (1.5)$$

This says that the shear is proportional to the radial component of the magnetic field, **B**, and the axial component of the rotor surface current density **K**. The current density will depend on **B** (generated by currents in the stator), the rate of change of **B** as seen by the rotating rotor, and the mutual inductance of the stator and rotor windings, which is purely a function of the geometry of the motor.

1.3.2 Mathematical Modeling

SatCon has developed software that calculates the performance of the induction machine [7]. The model uses the geometry of the machine to calculate the mutual inductances of the rotor cage and the stator windings. From that, it can determine what magnetic flux is produced by the stator windings and thus what currents are induced in the rotor. The magnetic flux, Λ, induced by a current carrying wire is proportional to the current:

$$\Lambda = LI \qquad (1.6)$$

The constant of proportionality, L, is the inductance of the loop and is solely a function of geometry. The flux is simply the magnitude of the flux density, B, times the area of the loop. The inductance of a rotor loop is comprised of a space-fundamental component, describing the flux which couples the rotor and stator and thus produces power, and a leakage component,

which takes into account flux produced by rotor and stator currents which is not mutually coupled. Thus the inductance of the rotor is [6]:

$$L_r = \frac{3}{2}(\wp_{ag}k^2N^2) - L_l \tag{1.7}$$

Where L_r is the total inductance of the rotor, L_l is the leakage component. The first term on the right-hand side is the fundamental component. For the fundamental component, N is the number of rotor bars, k is a winding factor which is a function of the angle between the rotor bars, and $\wp_{ag}$ is the air gap permeance. The permeance of the air gap is a measure of how well flux can cross the gap between the rotor and the stator [6]:

$$\wp_{ag} = \frac{4}{\pi}(\frac{\mu_o Rl}{p^2 g}) \tag{1.8}$$

Here, R and l are the rotor radius and length, respectively, p is the number of poles and g is the effective gap length. The effective gap length is usually more than the physical gap length due to irregularities on the surfaces of the rotor and stator which affect the permeance of the gap. Rotor currents can thus be found by calculating the flux produced by the stator, and by using the geometry of the machine to calculate inductance.

With the currents on the rotor known, power developed across the air-gap between the rotor and the stator is given by:

$$P = \frac{3|I_r^2|R_r}{s} \tag{1.9}$$

where P is the power developed, the factor of three comes from the three phases in the machine, I_r is the rotor current (obtained from the fluxes and the inductances), R_r is the rotor

resistance (obtained from geometry) and s is the slip. The slip is an expression of the difference in speeds between the rotor and the stator. It is given by:

$$s = \frac{\omega_r}{\omega} \qquad (1.10)$$

Here, ω_r is the rotor electrical frequency and ω is the stator electrical frequency. The electrical frequencies are the frequencies at which the **B**-field rotates. For most machines, the slip at a point near the maximum-torque point is around 0.05. If the rotor and stator frequencies were the same, $\frac{\partial \mathbf{B}}{\partial t}$ would be zero and there would be no electric field and thus no current density in the bars. This implies no torque.

The electrical frequency of the stator is a function of the frequency of the applied current and the number of pole pairs (i.e., in the previous section, the number of poles would be the number of current loops to which each phase is routed). Due to the phase lag inherent in Faraday's law (i.e., the time derivative of a sinusoid is an out of phase sinusoid), the rotor field will lag or lead the stator depending on whether the machine is being used as a motor or a generator. The relation between these electrical frequencies and the mechanical speed is:

$$p\omega_m = \omega - \omega_r \qquad (1.11)$$

where p is the number of poles and ω_m is the mechanical frequency.

A more detailed explanation of the mathematical modeling of an induction machine is beyond the scope of this thesis. It would include more detailed explanations of how mutual inductances are derived from geometry and how the magnetic field and flux densities through the current loops are calculated using Fourier expansions of the fundamental **B**-field. What is important to this thesis is to understand what is being modeled and how, and to have a tool to

evaluate the effects of changes in material properties and geometry on machine performance.

In Chapter Three, a change in geometry required to simplify manufacturing will be analyzed

using the concepts developed here. A Matlab code was used for the manufacturing analysis of

this machine.

1.4 References

[1] Pasquarella, G., & Reichert, K. (1990). Development of Solid Rotors for a High-Speed Induction Machine with Magnetic Bearings. Technical Report. Zurich: Swiss Federal Institute of Technology.

[2] SatCon Technology Corporation. (1995). Annual Report. Cambridge, Mass: SatCon Technology Corporation.

[3] Baldor Motors and Drives. (1994). Stock Product Catalog 501. Fort Smith, AR: Baldor Electric Co.

[4] O'Handley, R.C. (1996). Unpublished Lecture Notes: Magnetic Materials. Massachusetts Institute of Technology, Cambridge.

[5] Slemon, G.R., and Straughen, A. (1980). Electric Machines. Reading, Mass: Addison-Wesley.

[6] Kirtley, J.L. (1995). Unpublished Lecture Notes: Mathematically Assisted Design of Electric Machines. Massachusetts Institute of Technology, Cambridge.

[7] Kirtley, J.L. (1994). MatLab script: Polyphase Motor Design Program MOTOR. Massachusetts Institute of Technology, Cambridge.

Chapter 2

CURRENT MANUFACTURING PRACTICE

2.1 Introduction

High power densities and high speeds put unusual demands on the mechanical design of electric machine rotors. High speed implies higher mechanical stresses in the core and cage of the rotor. It also requires tighter dimensional tolerances on rotor and stator diameters, concentricities, and slot dimensions. These constraints generally increase manufacturing costs by necessitating the use of higher strength materials and exacting machining and fabrication requirements. High power density implies higher operating temperatures, higher current densities, and the use of higher permeability magnetic materials. These increase cost by requiring high-temperature materials, a copper squirrel cage, and aggressive cooling schemes.

The following two sections will put the manufacturing problem in context. Section 2.2 will summarize current industrial practice which is able to fabricate low cost, low strength, low power density rotors. It will be shown that these processes are incapable of making a high performance rotor cost-effectively, if at all. The current fabrication techniques used by SatCon will be the subject of Section 2.3. While SatCon's current technique can address some materials choice issues, it is unable to form these materials optimally.

2.2 Conventional Industrial Manufacturing Practice

Figure 2.1 shows the basic production flow for conventional rotors for induction

machines. The geometric and material properties limitations that each process imposes

on the final product will be dealt with in turn.
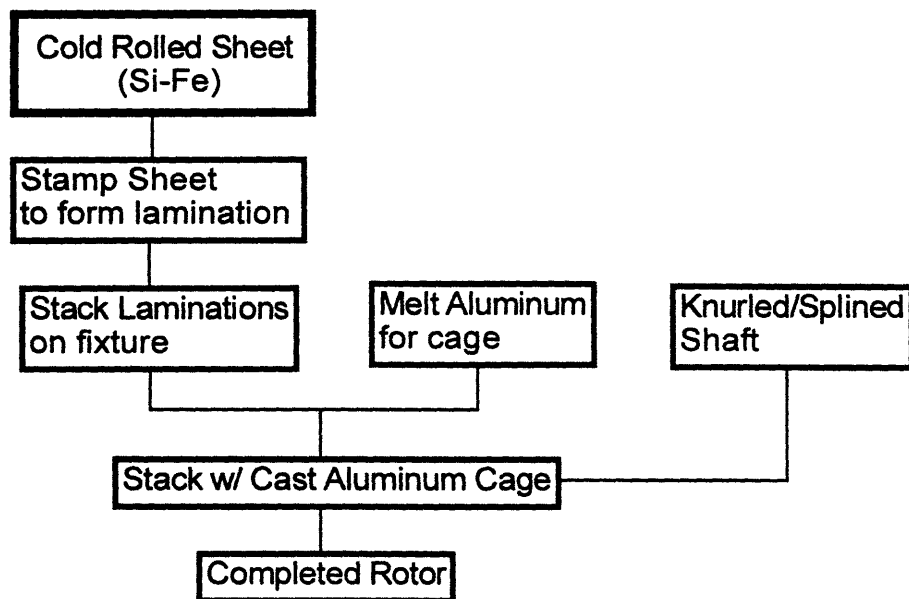
Figure 2.1. Conventional rotor production sequence

A typical, final-assembled rotor is shown in Figure 2.2. The core appears solid,

rather than laminated, for clarity. The impellers on either end are used for cooling and

serve as the end rings which short the bars of the cage together. The bars, being

embedded in slots in the core, are not visible.
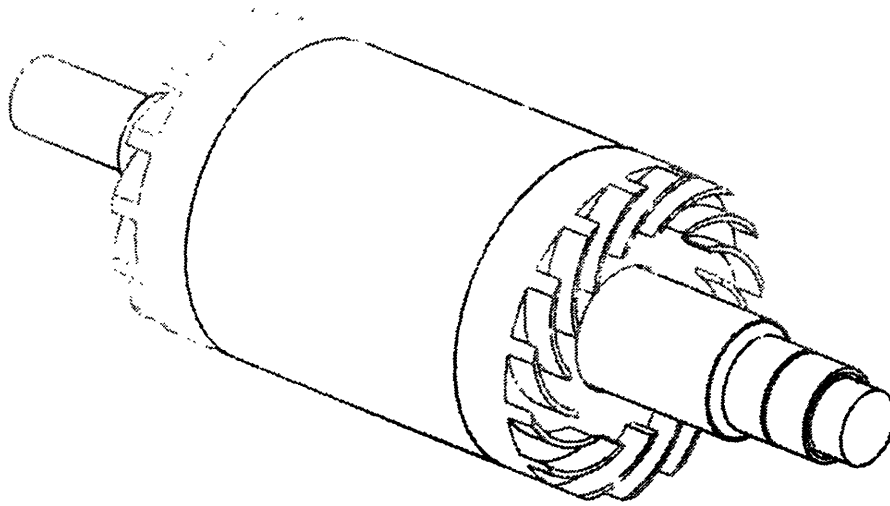
Figure 2.2. Typical Fully Assembled Rotor

2.2.1 Cold Rolled Sheet

The laminations comprising the magnetic core of the rotor must be blanked from rolled sheet. The rolling process introduces a lower limit on the thickness of laminations that can be used (of about 0.1mm thick) [1] and increases the brittleness of the material due to cold working. The material most commonly used for fractional horsepower motors is low carbon steel. For somewhat higher horsepower applications, where core losses necessitate the use of a magnetically softer, lower conductivity material, iron alloyed with 0.5wt% to 3.5wt% silicon is used. Silicon lowers the electrical conductivity of the iron, leading to lower eddy current losses during operation of the motor. Common motor applications use 24 to 29 gauge (0.6mm to 0.343mm, respectively) laminations [1].

Lower core losses are obtained using "thin" lamination sheets, of 0.1-0.17mm thicknesses [2]. The mechanical strength of silicon-iron is adequate for most low speed applications, having ordinarily a yield strength of around 380 MPa. Cold rolled silicon irons typically have tensile strengths of around 413-448 MPa [1]. A conventional 75 kW motor has a rotor diameter of about 50 cm and a rotational speed of 3600 rpm, maximum [3]. The inertial stresses induced are a maximum on the inner diameter of the rotor and are about 180-200 MPa.

2.2.2 Blanking Process

The rolled sheet must be blanked to a particular shape, stacked to the proper height, and fastened together by riveting, bolting, welding, or the use of an adhesive. The sheet is blanked in either a progressive or a single station die. The former is used for high volume applications and has the disadvantage of being inflexible. The single-station die is used for shorter production runs and the shape of the lamination can be changed more easily. A progressive die sequence producing both rotor and stator laminations is shown in Figure 2.3.

Material removed in station 1 ■, 2 ▨, 3 ▢, 4 idle, 5 ▩
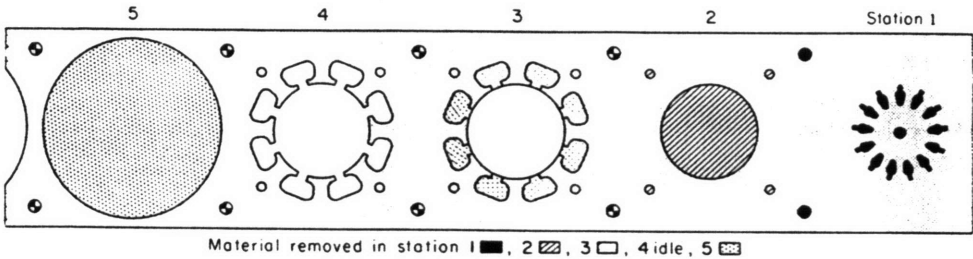
Figure 2.3. Progressive die sequence [4]

The blanking process is basically a shearing process. It introduces burrs at the edges of the lamination and harms the flatness of the sheet. The dimensional tolerances available from a typical progressive die are as follows. The thickness of the sheet has an error of ±0.05mm, burr size has a maximum around 0.05mm and the tolerances on other dimensions are ±0.05mm per mm of the dimension in question [5].

Excessive burrs can lead to stacking difficulties, and can provide an axial conducting path across sequential laminations, degrading the efficiency of the core. Stacking warped laminations leads to gaps between the laminations. These gaps represent lost volume of magnetic material in the core. This lost volume can increase the necessary stack length by up to 10% [5]. To make up for this, cores must be longer to contain a given volume of magnetic material. This is especially true for thin laminations, where flatness is more difficult to maintain and burrs are larger relative to total thickness. The loss of volume is expressed as a stacking factor, which is the ratio of actual volume of iron to the measured stack length times its cross sectional area.

2.2.3 Casting the Aluminum Cage

After the stack has been assembled and fastened, the conducting bars are poured directly into the rotor slots to form the squirrel cage. Vertical and horizontal cold chamber die casting are the most commonly used processes to perform this task. The former is used more often for larger motors while the latter is used for smaller (fractional

26

horsepower) motors. Centrifugal and permanent mold casting are also used to a lesser extent.

To obtain a good casting, the laminated stack must be assembled accurately, be free of burrs, and be placed properly in the mold cavity. Burrs create turbulence in the flow of molten aluminum and lead to voids. Proper placement of the stack in the mold helps ensure fewer cracks and inclusions in the bars due to shrinkage and differential thermal expansion between the stack and the bars.

The aluminum alloys used are primarily the rotor alloys specified as 100.0, 150.0, and 170.0. They are 99.0%, 99.5% and 99.7% pure aluminum, respectively. More impurities in the aluminum make casting easier in terms of better crack resistance and less shrinkage. However, higher impurities mean lower conductivity. For instance, rotor alloy 170.0, the purest of the rotor alloys, has an electrical conductivity of 60% IACS (International Annealed Copper Standard) at room temperature. This number changes only slightly for the remaining two alloys, down to 56% IACS for the 100.0 [6]. Commercially pure copper, in comparison, has an electrical conductivity of 0.568 ($\mu\Omega$-cm)$^{-1}$, which is defined as 100% IACS [7].

Due to its low conductivity and strength (relative to copper), the use of aluminum as the squirrel cage material clearly puts a limitation on the speed and power density of the induction machine. So why not cast copper bars into the rotor as is done for aluminum? There are several problems with this idea. The aluminum casting alloys melt at around 580°C while copper alloys melt at about 1080°C. This makes it very difficult to cast the copper into the stack without premature freezing and resulting voids.

27

If made of silicon iron, the stack in the magnetically annealed condition can only be raised to around 750 °C before seeing degradation in its magnetic properties. So it is quite possible that a melt of 1100 °C copper would at least locally degrade the properties of the stack.

In spite of these difficulties, one company, THT Presses, does have a patented copper squirrel cage casting technique. Since the technique is proprietary, it is unknown exactly how the problems are overcome. The process has been described as a modification of the high-pressure vertical die casting process commonly used for aluminum (Ted Thieman, personal communication, July, 1995). The results of the process will be described in more detail in Section 3.5.

2.2.4 Shaft Insertion

Most shafts in conventional motors are centerless ground bar stock, inserted using a spline and a thin layer of epoxy resin to resist spline corrosion and eliminate the gap between the shaft and the core. The formation of the spline does require an extra broaching operation on both the rotor core (internal) and on the shaft itself (external). The broaching operation is a fast, accurate process which produces a reasonably good surface finish on both the internal and external faces.

Tolerances required on the spline are not all that tight. For instance, on a 10 kW motor with a 25.4mm shaft, the tolerance on the major diameter of the spline is +0.76mm, -0.00mm [8]. This is not difficult to achieve.

2.2.5 Summary: The Limitations on Motors Imposed by Current Practice

The limitations of current industrial practice can be listed as follows:

• Strength Limitations: silicon iron laminations typically have yield strengths around 380 MPa with tensile strengths around 413-448 MPa, making them relatively weak and brittle. The more costly cobalt iron laminations used for some high performance applications can have yield strengths upwards of 520 MPa [9]. This still puts a severe limitation on the rotational speed of a motor of sizable radius. Additionally, the aluminum used in the cage yields at 100 MPa, potentially making it the strength-limiting material.

• Electrical Performance Limitations: The aluminum used for the squirrel cage has an electrical conductivity of less than 60% IACS while even high strength copper alloys have conductivities of above 85%.

• Dimensional Limitations: The dimensional accuracy of the stack is limited by both the stamping and the stacking processes. For example, the inaccuracies are such that on a 76mm round stack, the OD cannot be held to better than ±0.25mm [5]. For a high performance machine this can be 50% or more of the design air gap.

• Cost Limitations: the stamping process used to make the laminations is very capital-intensive and is only cost effective in large volumes. It is also expensive to change geometry.

2.3 Current Practice at SatCon

SatCon's method to date of manufacturing high performance electric motors has addressed several of the materials choice issues that limit the performance of conventional motors. However, since SatCon has been involved primarily in making prototypes, the materials are not formed optimally. The following sections describe the materials substitutions currently made by SatCon to overcome the shortcomings of low power density machines.

2.3.1 Magnetic Core

The choice of magnetic core material for a high power density motor is primarily dictated by strength considerations. According to finite element analyses performed at SatCon, for a motor with rotational speeds of 60,000 rpm and a diameter of 110mm (e.g., the SatCon low speed turbine alternator), the stresses on the inner diameter of the core can be upwards of 1450 MPa. These stresses rule out the use of silicon iron or cobalt iron laminated cores. The metals are simply too weak, and the lamination of the core dangerously decreases the stiffness of the core/shaft. This leads to the fundamental shaft mode being at frequencies very close to the rotational speed.

Some of the lower surface speed motors can use the higher strength but more expensive Co-Fe alloys. Even these alloys, however, are too weak for the very high stress applications. For these, the solid rotor material Aermet 100 (Aermet) [11.1% Ni, 13.4% Co, 3.1% Cr, 1.2% Mo, 0.23% C, balance Fe, all weight percents] is used [10].

Aermet, though it has inferior magnetic properties, has a yield strength of upward of 1725 MPa, giving it more than adequate strength for even the most demanding applications.

Both of these alloys are formed using the Electric Discharge Machining (EDM) process for final shaping. In the case of Co-Fe alloys, this is done because the material is very brittle, and thus sensitive to vibratory cutting forces. In the case of Aermet, EDM is used as a finishing operation because the toughness of the material makes it difficult to machine conventionally, and because of the complex shape of the slots. Tolerances on the core are very tight since everything that gets assembled to the core (e.g., bars, end rings, shaft and cooling mechanisms) are press fit to it. Another advantage of EDM, especially when used to form magnetic alloys sensitive to heat treatment, is the relatively small heating zone in comparison to conventional machining. Unfortunately, EDM has a relatively slow material removal rate, making it less than optimal for volume applications [11].

2.3.2 The Glidcop Squirrel Cage

SatCon uses a cage of machined Glidcop bars instead of a die cast aluminum cage. Glidcop is a patented, dispersion-hardened copper alloy [Cu/Al_2O_3], made by mixing copper powder with particles of aluminum oxide and sintering the product. The oxide particles both strengthen the copper and allow it to maintain its properties at high temperatures of up to 700 °C. It has higher strength than pure copper and maintains its electrical and mechanical properties even after prolonged exposure to high temperatures [12]. The highest operating temperature of SatCon's motors is 200 °C.

31

The highest stresses in the squirrel cage are those arising from centrifugal forces. Like the magnetic core, these stresses are highest at the inner diameter of a rotating toroid. Thus they are found at the inner diameter of the end rings. For example, the stresses on the inner diameter of the 76mm OD - 38mm ID end ring found on the SatCon starter-generator induction motor are around 310 MPa. This is far above the yield strength of aluminum and a little above that of pure copper.

Glidcop has superior strength at some sacrifice of electrical conductivity. There are three grades of Glidcop, reflecting three concentrations of the aluminum oxide particles that strengthen the material. As the volume of alloying particles increase, the strength increases and the electrical conductivity decreases. Hence the grade with the highest strength (AL-60) has a yield strength of 503 MPa and an electrical conductivity of 78% IACS while the grade with the lowest strength (AL-15) has a yield of 310 MPa and a conductivity of 92% IACS [12].

To fabricate the squirrel cage, the Glidcop is machined to very exacting tolerances and press fit into the slots of the core. The end rings are machined and press fit to the bars. To ensure continuity of electrical conductivity from the bars to the end rings, the assembly is brazed with a silver-based alloy. To prevent the diffusion of silver into the bulk of the Glidcop, which would lower both the strength and electrical conductivity of the cage, the Glidcop must first be electroplated, making the brazing procedure complicated.

2.3.3 Shaft and Cooling Mechanisms

The shafts of SatCon's motors are fabricated and assembled in two ways. Some motors' shafts are centerless and cylindrically ground bar stock shrunk fit into the core. Other shafts are machined integrally with a machined core. Cooling mechanisms vary from motor to motor depending on whether they are water or air cooled. Air cooled rotors have machined impellers of 4340 steel press fit onto the end rings on either side of the rotor (Figure 2.4). Water cooled rotors have machined, 4340 steel water impellers called Barsky pumps press fit onto either end (Figure 2.5). The pump provides a pressure rise at one side of the rotor and a drop at the other in the fashion of a compressor/turbine pair. The water flows through axial holes in the rotor.
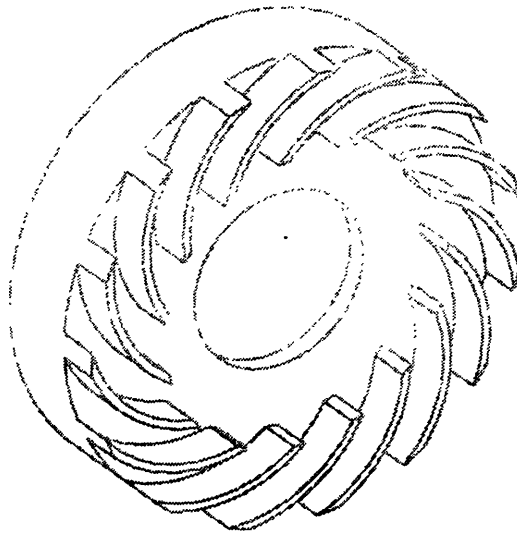
Figure 2.4. Impeller for an air-cooled motor
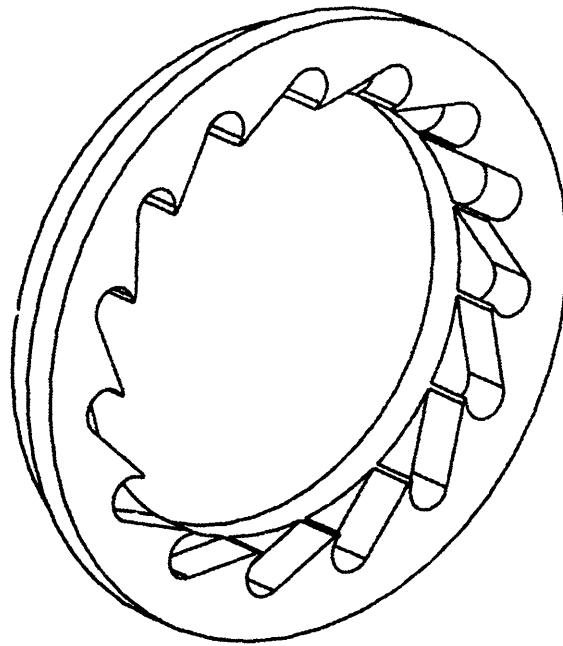
Figure 2.5. Barsky pump for a water-cooled motor

2.3.4 Summary: Problems Solved by SatCon Current Practice

The main problems that have been solved by SatCon involve using higher

performance materials for higher performance motors. High speeds require high strength

materials for the magnetic core and the squirrel cage. High power densities require high

conductivity materials and materials that can operate adequately at high temperatures.

These problems have been addressed by materials substitutions.

The problem of optimal forming of the materials remains. Currently, all parts are

machined and mechanically press fit together. The materials are slow to machine,

especially to the tight tolerances required for mechanical fitting. This main problem will

be addressed in Chapter Three.

2.4 References

[1] Metals Handbook (1990). Metals Park, OH: American Society for Metals.

[2] Arnon Data Sheet (1995). [Arnold Engineering Company]: Marengo, IL. Arnold Engineering Company.

[3] Stock Product Catalog 501 (1994). [Baldor Motors and Drives]: Fort Smith, AR. Baldor Electric Co.

[4] ASM Handbook, Vol. 14: Forming and Forging (1995). Materials Park, OH: ASM International.

[5] Tempel Steel Services Division (1993). [Tempel Motor Laminations]: Niles, IL Tempel Steel Company.

[6] ASM Handbook, Vol. 2: Non-ferrous Materials: Properties and Materials Selection Guide. (1995). Materials Park, OH: ASM International.

[7] Avallone, E. A. (ed.) (1987). Mark's Standard Handbook for Mechanical Engineers, 9th ed. New York: McGraw-Hill.

[8] Machinery's Handbook. (1994). New York: Industrial Press.

[9] Alloy Data Sheet: Hiperco 50 HS (1995). [Carpenter Steel Division]: Reading, PA. Carpenter Technology Corporation.

[10] Alloy Data Sheet: Aermet 100 (1995). [Carpenter Steel Division]: Reading, PA Carpenter Technology Corporation.

[11] Kalpakjian, Serope. (1995). Manufacturing Engineering and Technology. Reading, MA: Addison-Wesley.

[12] Glidcop: Copper Dispersion Strengthened with Aluminum Oxide (1994). [SCM Metal Products]: Research Triangle Park, NC. SCM Metal Products.

Chapter 3:

THE INDUCTION ROTOR MANUFACTURING PROCESS

3.1 Introduction

This chapter will describe the induction rotor manufacturing process in detail, describe its

inherent trade-offs, list the possibilities considered, and demonstrate some of general principles

of this kind of manufacturing process analysis. A generalized approach to devising the most

effective manufacturing process will be presented in Chapter Five.

Section 3.2 will give an overview and flow chart of the complete process. The sections

following will detail each step and each process considered. Section 3.3 will discuss the

functional decomposition of the rotor into its components. This conceptualizes the function of

each part to ensure no duplication of function across various parts and to focus the design so that

no parts or materials have properties or features that do not relate to their function. Sections 3.4

through 3.7 will describe the techniques and trade-offs involved in each functional component.

Section 3.8 will detail the chosen diffusion bonding assembly process.

3.2 Process Overview

A flow chart of the process is shown in Figure 3.1.

Proposed Process for Induction Rotor Manufacture

Bars/End Rings Cr-Cu Extrusions	Cast Magnetic Core Aermet 100	Cast Impeller Caps 410 Stainless	Bar Stock shaft 410 Stainless
Cut to length	No pre DB machining	No pre DB machining	Turned shoulder Cut to length

Pre-Diffusion Bond Assembly

Diffusion Bonding

Vacuum Heat Treatment

Finish Machining
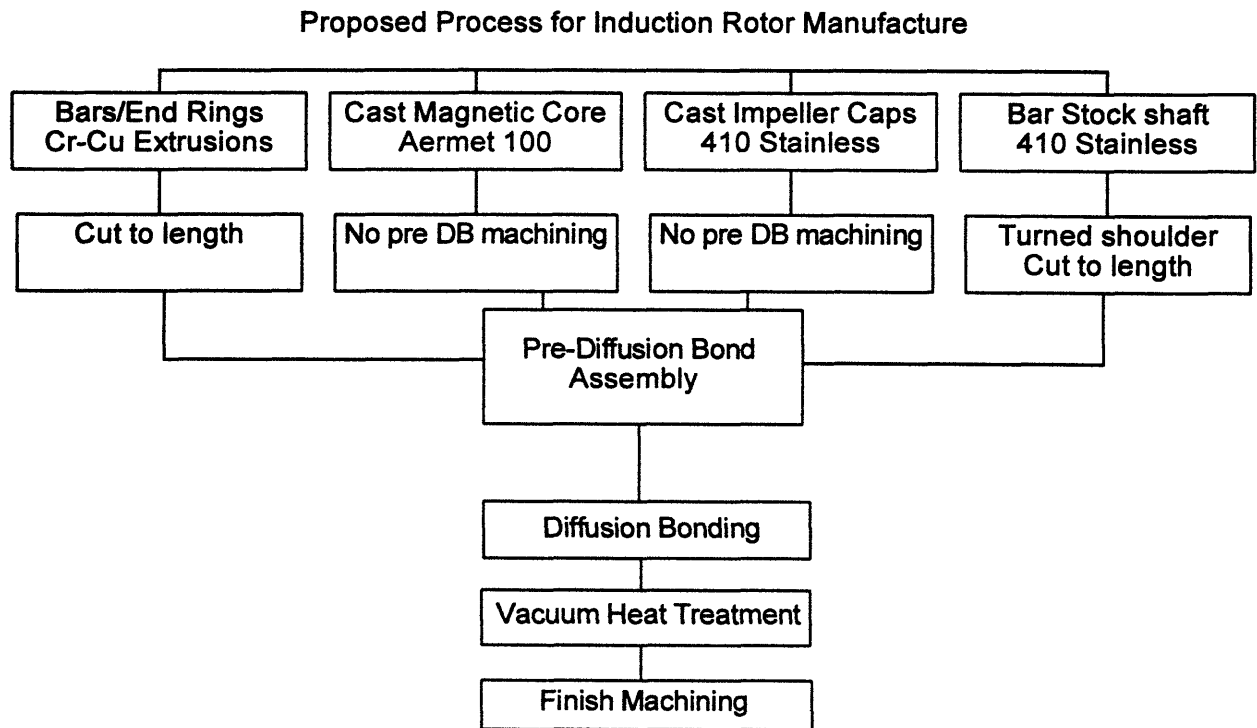
Figure 3.1. Final new production sequence for the high-performance induction rotor

The top row indicates the material, process, and initial form of each functional element of the rotor. Net shape processes are used to manufacture each element. They require minimal machining before assembly. Since the tolerances of parts produced by net shape processes are

37

generally higher than those of machined parts, the elements initially form a loose assembly. Final joining is accomplished through the diffusion bonding of the copper bars/end rings and impeller caps to the cast magnetic core using an electroless nickel interlayer. The entire assembly is then heat treated to optimize the electrical, magnetic, and mechanical properties of each material. Thus only one heat treat operation is used for the whole assembly, rather than for each part separately. Finally, the outer diameters (OD) of the rotor and shaft are ground to fit the stator and bearings.

3.3 Functional Decomposition

Functional decomposition of a part or an assembly separates the assembly into groups of parts with the same function. The function of each part is identified in the simplest terms possible for two primary reasons; they are to ensure that:

- unnecessary duplications of functions are eliminated, and

- parts do not contain features or have properties that add cost and do not relate to their function.

First, the function of the assembly as a whole must be stated (the starter/generator rotor assembly is shown in Figure 3.2). The function of the rotor is to produce mechanical power by the conversion of electrical energy.
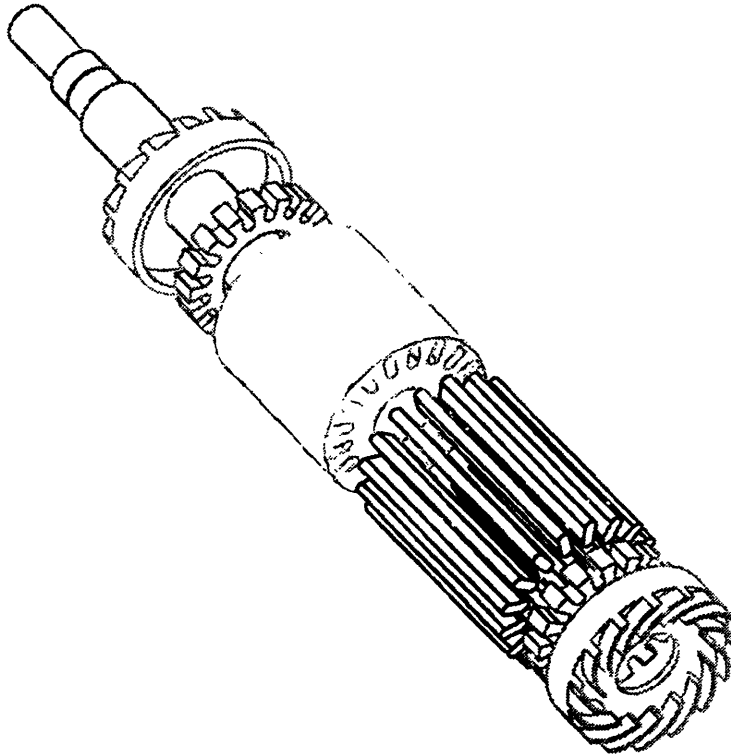
Figure 3.2. Exploded view of the rotor assembly

The rotor can be seen as the assembly of four components (Figure 3.2): the magnetic

core, the conducting squirrel cage, the cooling mechanism (in this case, impellers at either face of

the rotor), and the shaft. The function of each component is:

- *cage* - carries current induced by the stator to produce torque,
- *core* - transmits torque from the cage to the shaft, enhances torque produced by the cage
  (by increasing the magnetic flux density through the current loops),
- *shaft* - transmits torque from the core to outside the machine, and
- *impellers* - dissipates heat generated by losses in the conversion of electric to
  mechanical energy

A few design issues are immediately identified by the functional decomposition. The first is that there is a duplication of a function. The core transmits torque from the cage to the shaft and the shaft transmits torque from the core to outside the machine. This suggests that the core and the shaft should be manufactured integrally, as one piece. This possibility will be examined in the section focusing on core fabrication. It is, however, important that this issue was identified by the functional decomposition. That is precisely its purpose.

Another point to notice is that the decomposition reveals that the core merely needs to suspend the cage in the magnetic field. Usually this is done by geometrically constraining the bars using holes in the core. This is not the only solution, however. Other methods of joining the cage to the core should and will be considered.

Finally, the decomposition shows that the cage should not be made to bear anything but inertial loads. The core should be the torque-transmitting member.

The following five sections will demonstrate the details of how the fabrication process for each functional element was determined. A similar analytical process will be carried out for each element. First, the performance requirements of each element will be explained. These are obtained from the functions of each element and translated into engineering specifications. Second, the assembly requirements will be enumerated. This explains how the part needs to fit into the entire assembly. Both the performance and the assembly requirements are listed explicitly as guidelines to which the manufacturing and joining processes must conform. Finally, the various manufacturing process possibilities will be listed and discussed. An optimum process will be arrived at for each part and for the assembly as a whole.

3.4 The Magnetic Core

3.4.1 Performance and Assembly Requirements

As was seen in the functional decomposition, the function of the magnetic core is to suspend the cage in the magnetic field, enhance the magnetic flux through the cage bars, and transmit torque. The primary material properties required of the core are therefore mechanical and magnetic. To be more specific, the mechanical properties required are primarily high yield strength and high stress-rupture strength. Stress-rupture strength is the applied stress necessary to cause rupture in a specified time, usually 1,000 hours or 100,000 hours [1]. Magnetic properties necessary for successful operation are high saturation induction, high permeability, high electrical resistivity, and low AC (alternating current) core loss. Saturation induction is the highest magnetic flux density possible in a material, when all the magnetic moments in the material are aligned with the applied field. Permeability is the ratio of the magnetic flux density obtained for a given applied magnetic field. It is roughly linear until saturation is reached.

The assembly requirements for the core are two-fold: the cage must be held to the core and the core must also be held to the shaft.

Two cores are shown in Figures 3.3 and 3.4. One is the starter/generator core and the other, more unusual, configuration is that of the traction motor (a photograph of which was given in Figure 1.1). The original starter/generator core was a laminated Co-Fe stack. The laminations are not pictured here for clarity.
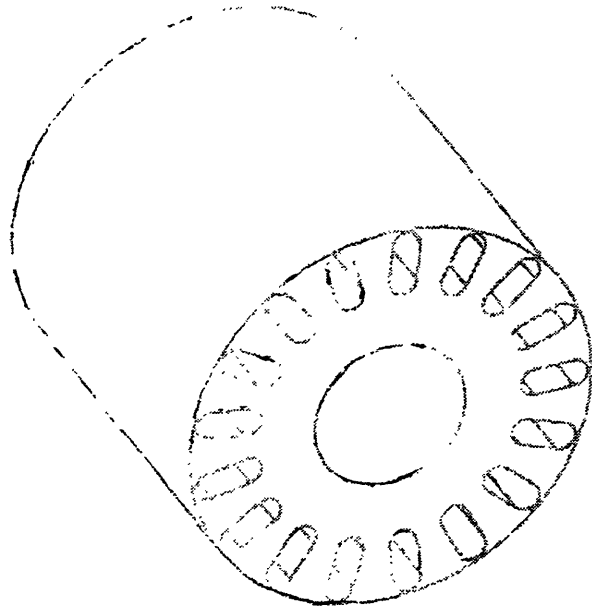
Figure 3.3. Starter/Generator motor magnetic core
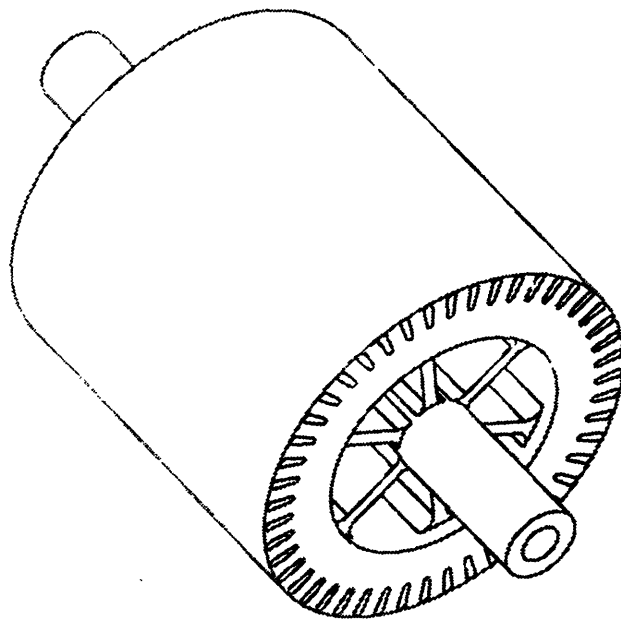
Figure 3.4. Traction motor magnetic core with integrally machined shaft

3.4.2 Materials Possibilities

In contrast to a conventional induction motor, the limiting material property that almost by itself dictates core material choice for a high speed machine is mechanical strength. The maximum stress in a spinning cylinder is the tangential stress (hoop stress) on the inner diameter generated by inertial forces. This maximum stress is [2]:

$$\sigma_t^{max} = \rho v^2 \frac{(3+\upsilon)}{4}\left[1 + \frac{(1-\upsilon)}{(3+\upsilon)}\left(\frac{r_i}{r_o}\right)\right] \tag{3.1}$$

where ρ is the material density, v is Poisson's ratio, v is the tip speed and r_i and r_o are the inner and outer radius, respectively. Since density and Poisson's ratio are quite similar (within 10% of each other) for most materials considered, the dominant term in Equation 3.1 is the tip speed. The ratio of inner to outer radius has little effect unless the rotor has no interior hole (e.g., an integral shaft/core) in which case the maximum stress is decreased by a factor of two [2]. For example, the tip speed of the high speed alternator, which has a diameter of 66 mm and runs at a design speed of 100,000 rpm, is 345 m/s. The stress on the inner diameter of the core is 1450 MPa.

The only magnetic alloys with the necessary strength are the cobalt-irons (for some of the lower tip speed applications) and Aermet. Not only are the cobalt-iron alloys five times as expensive as Aermet ($50/lb compared to $10/lb for Aermet, based on a quote from Carpenter Technology Corporation), but they are only available in sheet and are difficult if not impossible to cast effectively due to segregation of phases during cooling. An additional problem with the

Co-Fe alloys is that their magnetic properties are severely damaged at temperatures above 870 °C
[3]. This limits manufacturing and processing options.

3.4.3 Design for Net-Shape Fabrication: The Solid Rotor with Open Slots

The main issue to be dealt with regarding the form of the magnetic core is the necessity
of using a solid, rather than laminated, core. While cores are laminated to reduce eddy current
losses and improve the performance of low tip speed machines, stresses in high tip speed rotors
are too high for a laminated core. It seems the use of a solid rotor is unavoidable for high stress
applications. For a solid rotor, the eddy currents induced by the field on the rotor surface will
increase, degrading the efficiency of the machine. Since some axial currents will be induced in
the rotor, torque will increase at a given speed. Efficiency, however, will decrease.

There are ways to minimize the increased losses. One way is to reduce the ripple in the
field that the rotor encounters by closing the stator slots as much as possible [4]. Most
conventional stator slots are left wide open so that an automated winding machine can insert the
stator windings. In SatCon's designs, however, the stator slots are largely closed.

In order to use any net-shape process effectively in this application, another geometry
change must be made to the core. It will be necessary to "open" the slots of the core, making the
cross section of the core look more like a gear. Figure 3.5 shows the cross-sectional change.
This is done for two reasons. The first is that it would be very difficult to cast the thin walls
around the exterior of the slots, typical dimensions of which are shown in Figure 3.6. Unless
such a rotor were gated at the wall of every slot, which might require the gating of upwards of 30
slots, some slots would have voids due to premature freezing. Second, if a casting process were

44

used, closed slots (i.e., holes in the core rather than grooves in the surface) would require the insertion of cores in the mold. For the starter-generator rotor, as an example, this would mean the insertion of 17 cores in each mold. This would make the casting process excessively costly.
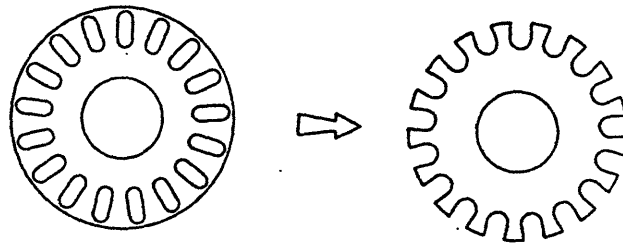
Figure 3.5. *Cross section of the original core (left) contrasted with that of an open slot core (right)*
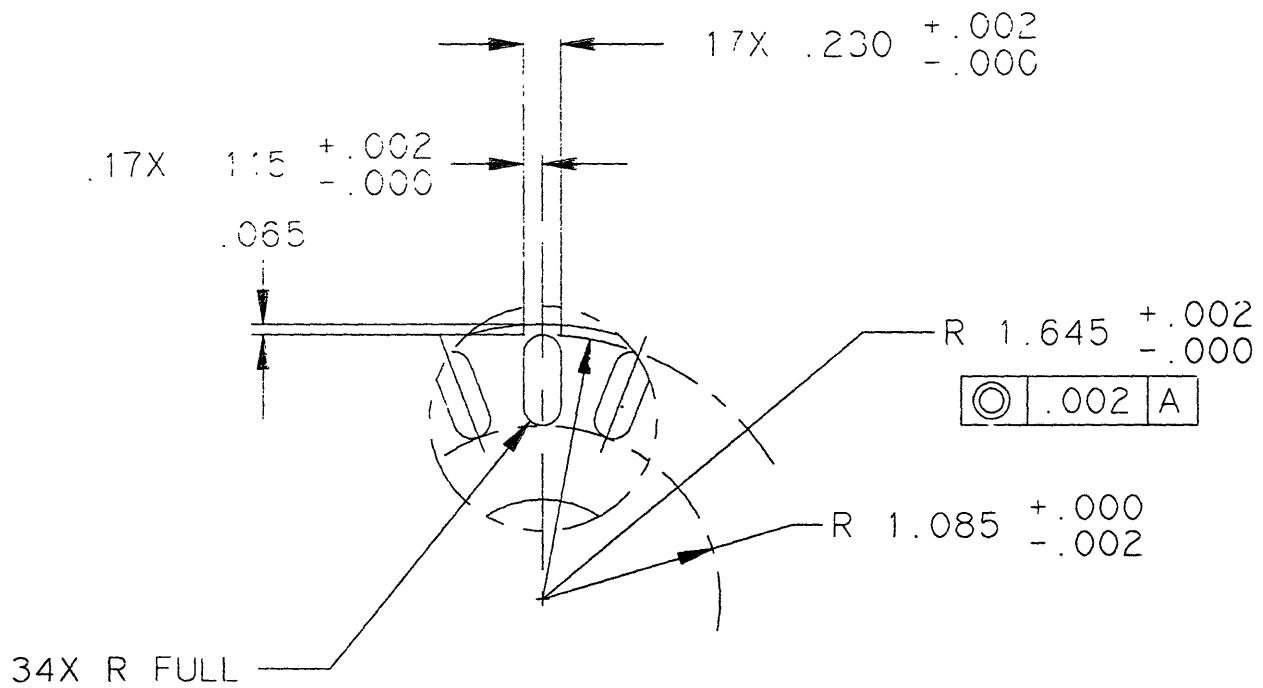
Figure 3.6. *Typical wall dimensions of a closed slot core (starter/generator geometry)*

The effect of open slots on motor performance must now be analyzed electromagnetically. The quantitative effect was calculated using the mathematical model embodied in the Matlab code described in Chapter One [5].

There are two competing phenomena in operation with respect to the opening of the slots: one which tends to improve performance (i.e., efficiency) as the slots are opened and one which tends to degrade it. The first is the decrease of leakage flux, expressed by a decrease in the leakage inductance of the rotor as shown in Equation 1.7. A decrease in leakage inductance results in an increase in total rotor inductance. If rotor inductance is higher, rotor current is higher for a given stator flux, as shown by Equation 1.6, and therefore developed power is higher according to Equation 1.9.

The second effect is flux concentration due to the presence of less iron. This latter effect is usually expressed as a larger equivalent air gap, which decreases the air gap permeance, $\wp_{ag}$ from Equation 1.8. A decrease in air gap permeance results in a decrease in rotor inductance, hence decreasing the current induced on the rotor, hence decreasing power.

Leakage flux is a magnetic flux that does not couple the rotor and the stator windings and therefore does not assist in the conversion or production of power [6]. Ideally, the path of least magnetic resistance (called the lowest reluctance path), is across the motor's air gap and through the current loops in both the rotor and stator. Figure 3.7 illustrates the mechanism of leakage. For a closed rotor slot (left), some of the flux produced by current in the rotor can go through the iron (a low reluctance path until the iron is saturated). This flux does not cross the air gap and couple to the stator, but it still requires power (i.e., rotor current) to create. For the open slot

46

(right) the lack of iron increases the reluctance of that path, reducing the amount of flux through it. More flux therefore crosses the gap and produces power.
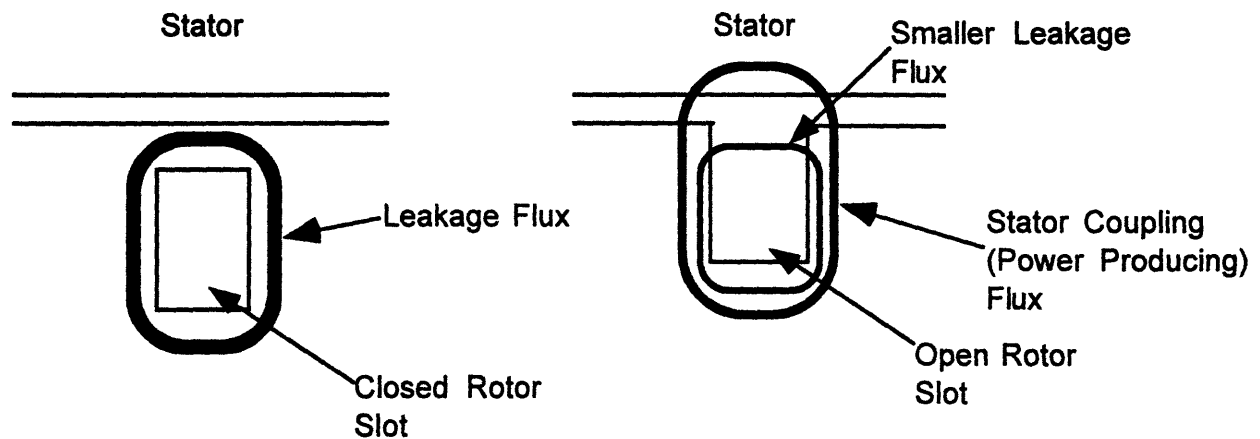
Figure 3.7. An illustration of the concept of leakage flux in an electric machine

The leakage inductance L_1 is proportional to the slot permeance, $\wp_{slot}$, which is given by [7]:

$$\wp_{slot} = \mu_o l\left(\frac{h_d}{w_d} + \frac{1}{2}\left(\frac{h_s}{w_s}\right)\right)$$

(3.2)

where l is the rotor length and h_d, w_d, h_g, and w_g are defined by the slot model geometry in Figure 3.8. For an open slot, $h_d=0$ so the slot permeance is reduced.
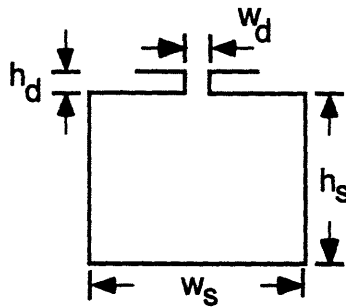
Figure 3.8. Slot model geometry (after [7])

Figure 3.9 illustrates the effect of flux concentration. When slots are closed, the flux can distribute itself uniformly across the air gap and be essentially radial. With open slots, the flux becomes concentrated in the teeth between successive conductors (conductors are not ferromagnetic and therefore are a high reluctance path for flux). The fringing has several negative effects: the iron gets closer to becoming saturated, increasing the reluctance of the path across the gap; the fringing creates components of **B** in the circumferential direction which are useless for creating torque; and leakage on the stator side of the gap is increased.

48

a) Closed Slots
Flux Uniformly Distributed

b) Open Slots
Flux Concentrated
Mostly in Teeth
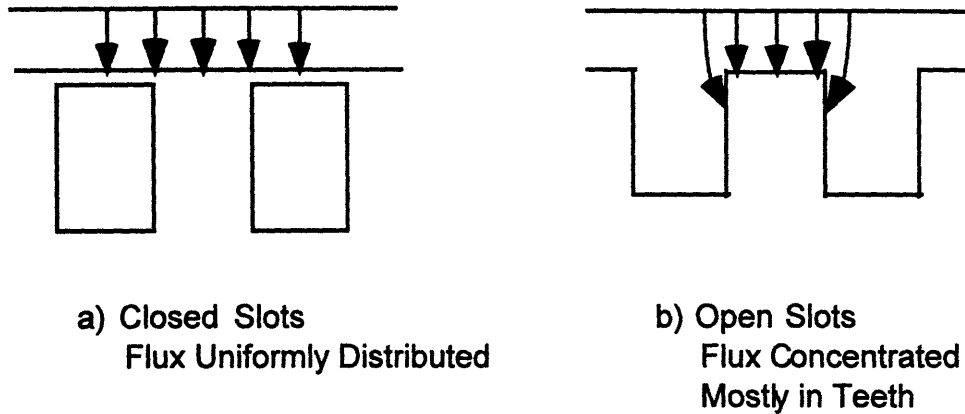
Figure 3.10. Flux concentration due to open slots (after [6])

The increased reluctance of the air gap is expressed as an increase in the effective length of the air gap by an empirically derived coefficient. The reluctance of any flux path is the reciprocal of the permeance and is given by a formula similar to that of electrical resistance:

$$R_m = \frac{L}{\mu A}$$ (3.3)

where L is the length of the path, A is its cross-sectional area and μ is its permeability.

In order to determine how these effects play out quantitatively, a numerical experiment was carried out using the Matlab code with the geometry of the (closed-slot) starter-generator. The geometry of the slot is modeled as was shown in Figure 3.8. To model an open slot, h_d was set to zero and w_d was set equal to w_s.

To run a comparison with the closed slot results, the total cross sectional area of the bars remained the same as the height and width were varied. Tooth flux density (i.e., the flux density in the iron around the slots) as a function of slot width is shown in Figure 3.10. The code calculates flux density from geometry (inductances), stator currents and an average permeability of the rotor iron. In reality, however, the permeability of a ferromagnetic material drops off to

49
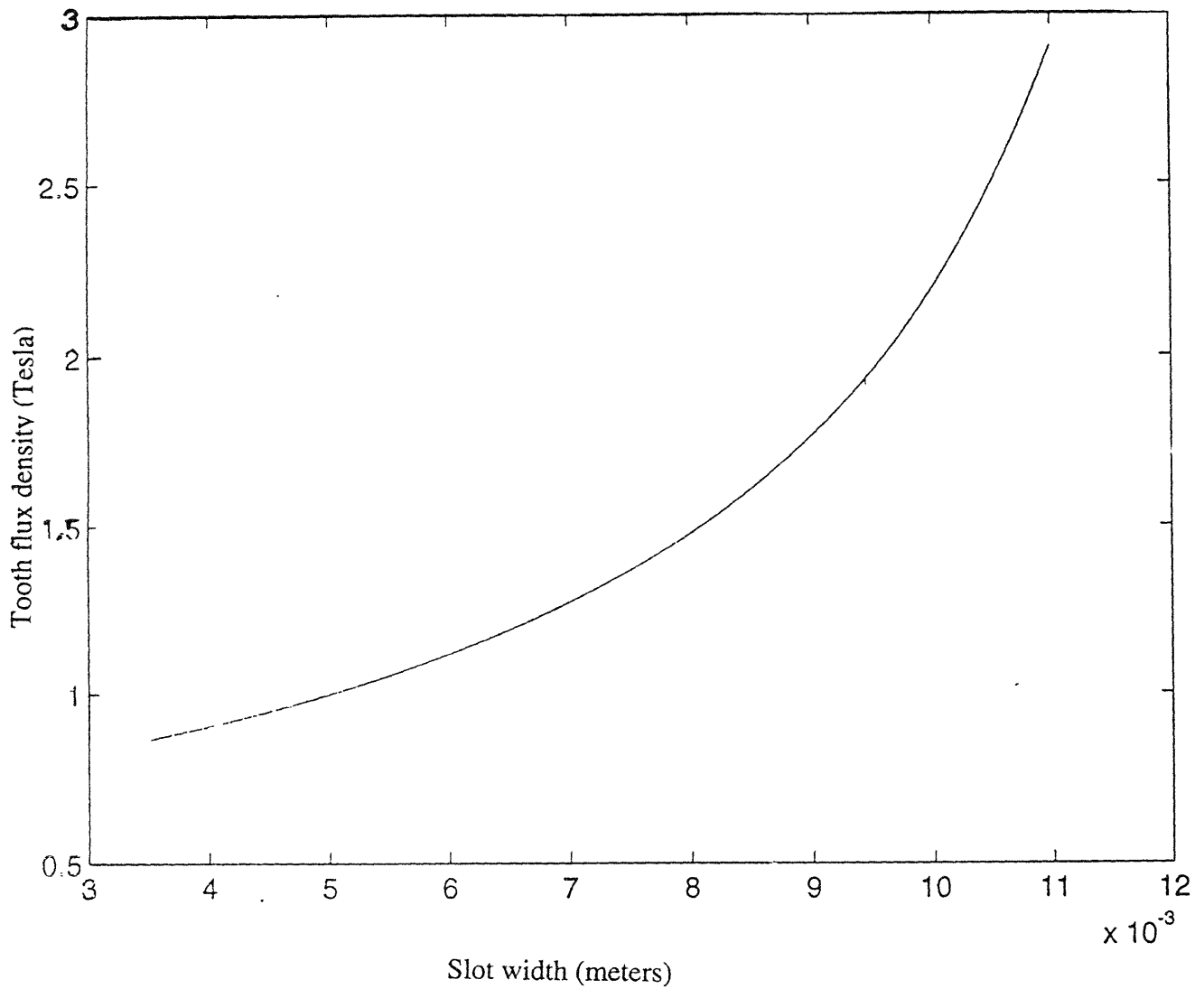
Figure 3.10. Tooth flux density vs. slot width for open-slot starter/generator rotor. The tooth iron is taken to saturate at 2 Tesla. The highest feasible slot width is thus about 9.5mm, as shown.
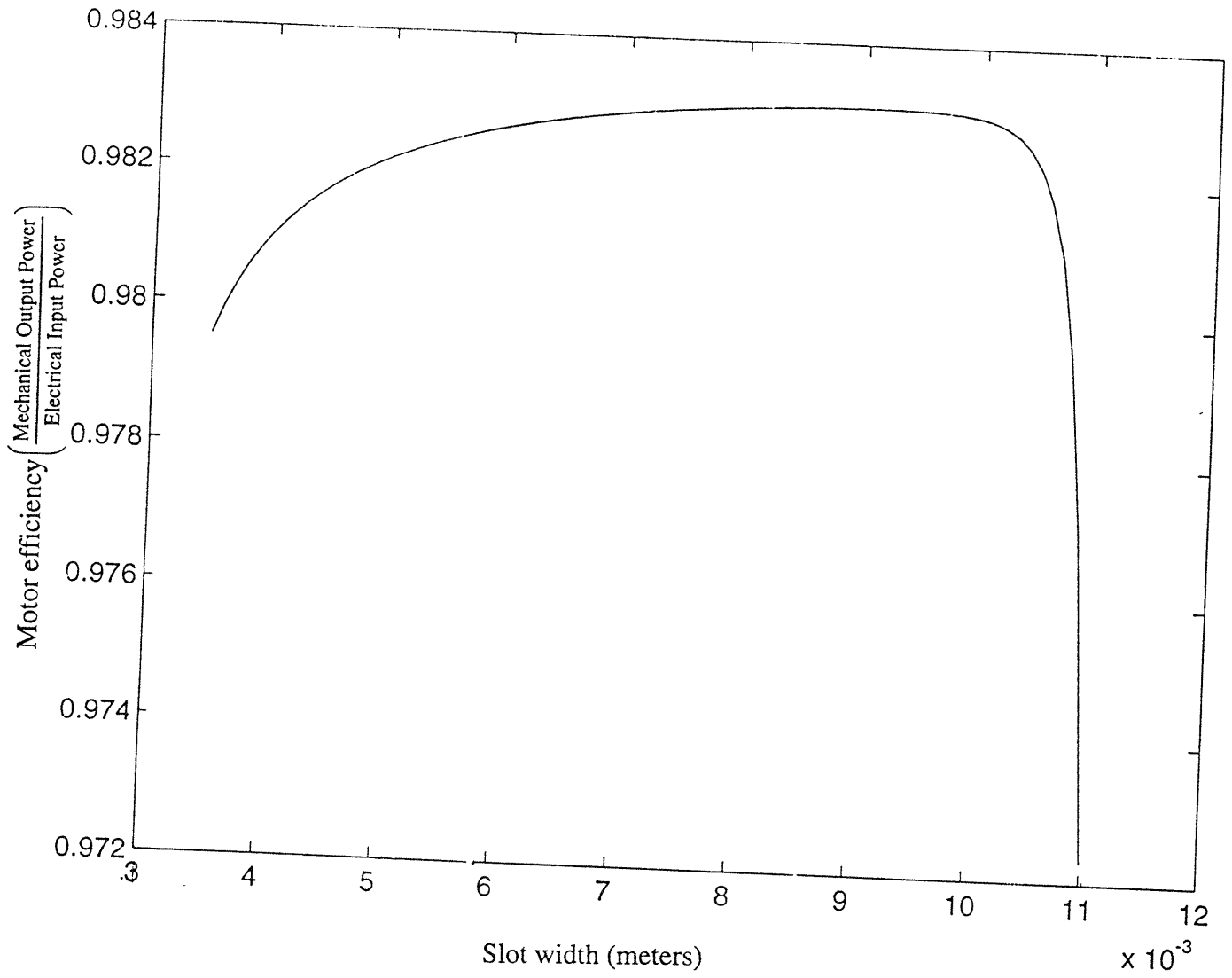
Figure 3.11. *Efficiency vs. slot width for the open-slot starter/generator rotor*
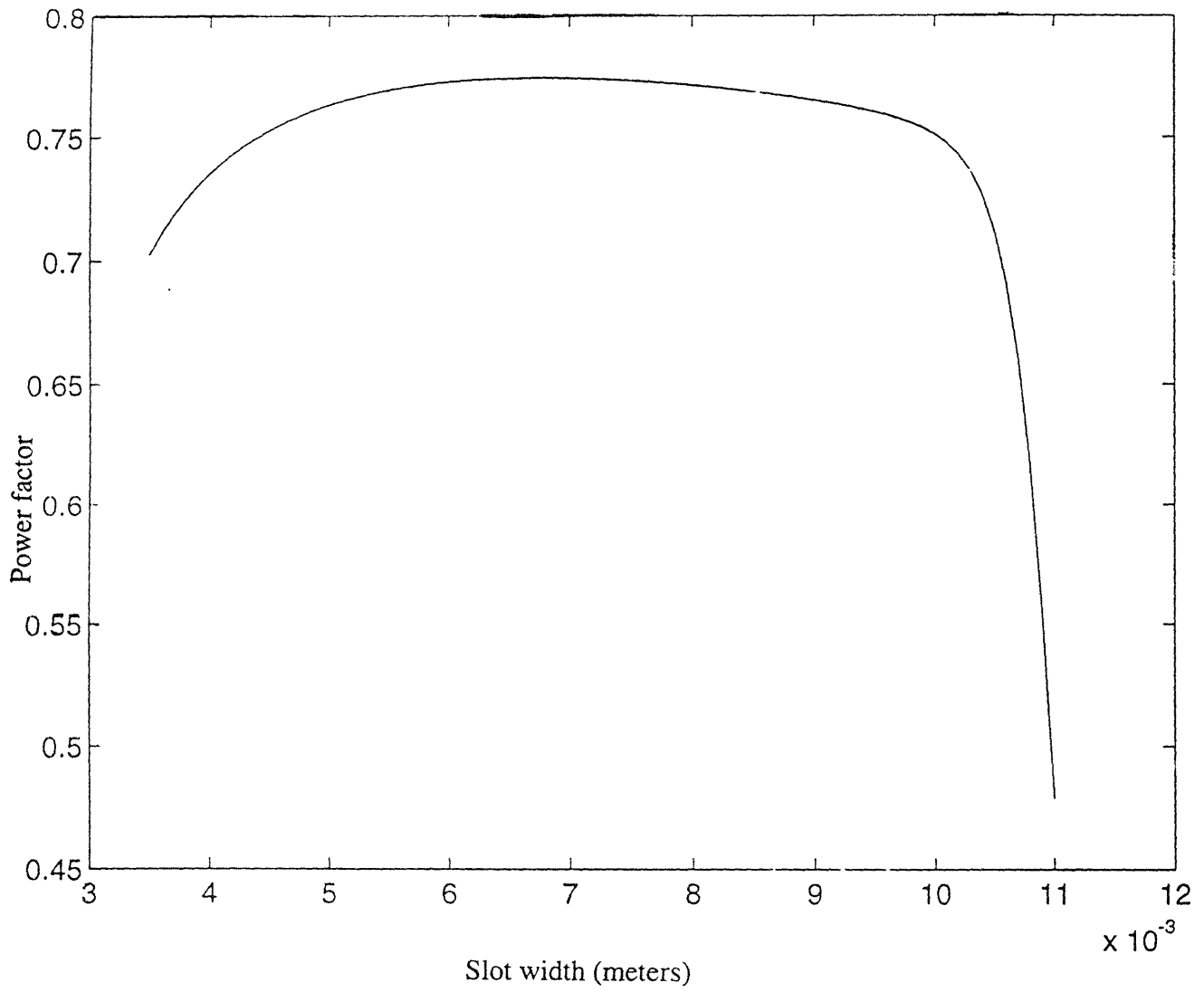
Figure 3.12. Power factor vs. slot width for open-slot starter/generator

nearly zero when the iron is saturated. As the slots become too wide (to the right of the plot), the teeth become too small and the iron is saturated at a flux density of about 2 Tesla. The slot width at which the flux density is equal to 2 Tesla is therefore the useful limit of the results. The effects on efficiency and power factor (an expression of the difference in phase between output voltage and current giving real power output) for the variances in slot width are shown in Figures 3.11 and 3.12. The efficiency and power factor of the original configuration were 98.2% and 75.3%, respectively.

It can be seen that the effect of opening slots is a second order effect. In the useful range of the plot (i.e., before the tooth iron saturates) efficiency varies by about 0.3% and power factor varies about 8%. As the conductors become too thin (on the left of the plot), leakage decreases while the increase in effective air gap increases faster, thus degrading performance. There is an optimum open slot width which is fairly close to the width of the original slots (about 8mm).

3.4.4 Net-Shape Fabrication Options

It seems, therefore, that the best option in terms of best performance at lowest cost is a solid Aermet rotor. The issue now becomes how to form it. Briefly, the options to be considered are: casting (investment, sand, or centrifugal), machining, powder metallurgy, forging, or extrusion. Powder metallurgy (PM) and extrusion can be ruled out immediately for similar reasons. Aermet is too strong and the cross-sectional area of the rotor too large to be extruded

cost-effectively, if at all. The press capacity required would be enormous. Aermet itself has never been extruded. It is similar, however, to some stainless steels in terms of composition and heat treatment so some comparisons can be made. In order to soften stainless steels for successful extrusion, most are heated to 815°C or above [8]. Due to the sensitivity of Aermet's properties to the presence of impurities [9], these temperatures would require the extrusion to be carried out in an inert atmosphere furnace, further adding to cost. In addition, the directionality inherent in the grain structure of an extruded product would adversely affect the magnetic properties of an extruded Aermet core by introducing axial anisotropy [10].

The cross-sectional area of the rotor is too large to compact the powder of a sintered product without a tremendous press capacity. An additional consideration for powder metallurgy is the length of the core. The length (upward of 150 mm for some rotors) would lead to density and other property gradients in the final product [11].

Several of the listed processes can be ruled out for other reasons. The core has a constant cross section, which would seem to make it ideal for centrifugal casting. Aermet, however, owes its good properties to tight control of impurities which requires the material to be vacuum cast. Although centrifugal vacuum casting should be possible in principle, it cannot be done with currently available equipment.
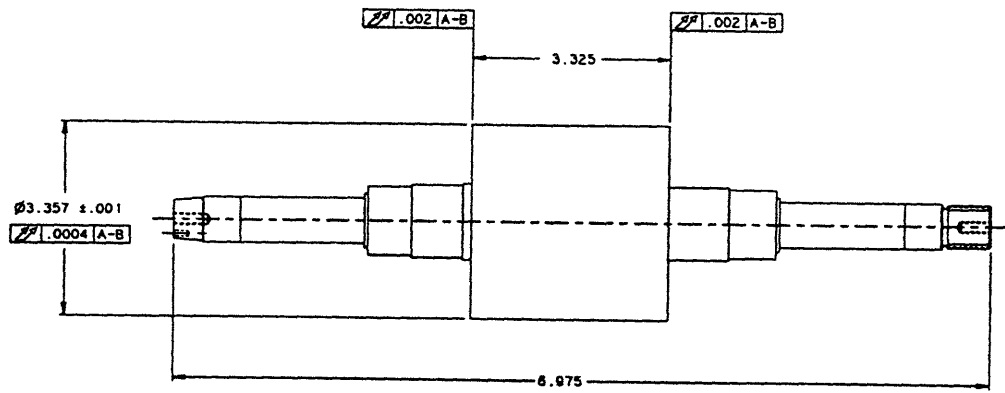
Figure 3.13. Integral shaft/core using representative dimensions (British units) from the starter/generator

The other issue, raised by the functional decomposition, is whether the core and shaft be constructed as an integral piece as in Figure 3.13. For the investment and sand casting processes the cost of the process is related directly to the largest dimension of the mold or die. In investment casting, for instance, each wax mold must fit onto the sprue. The more molds that can be fit on the sprue, the more cost-effective the process is. Since the shaft increases the length of the mold by about a factor of two, fewer molds can fit on the sprue, diminishing the effectiveness of the process. A similar argument can be made for the other processes. Since the shaft is such a simple geometry and can be bought from stock, it makes no sense to increase the size of the mold so dramatically to make such a simple piece. Thus, using a net-shape process to manufacture an integral shaft/core would be counter-productive.

3.4.5 Core Manufacturing: Conclusions

For strength reasons, a solid Aermet core must be used. The most cost-effective manufacturing process for this will be an investment, sand, ceramic, or resin mold casting process. For any of these processes, it is best not to cast an integral shaft/core. It will be necessary to open the slots in the core to use a casting process effectively. This has been shown to have a second-order positive effect on performance. Open slots will, however, create an assembly problem with the cage, since the bars will no longer be geometrically constrained. This problem will be addressed with diffusion bonding in Section 3.8.

3.5 The Squirrel Cage

3.5.1 Performance and Assembly Requirements

The squirrel cage is an efficient shape for providing several conducting loops through which a changing magnetic field passes to produce a current. Loops on SatCon's motors range from 17 to 48 copper conducting bars. Since their primary function is to conduct electricity, their most important material property is electrical conductivity, which should be as high as possible. The highest grades of aluminum that are conventionally used in induction machines have conductivities of only 58% IACS at room temperature. High performance applications would require at least a conductivity of around 80% IACS. This conductivity must not fall off precipitously when raised to the operating temperature of the motor, the upper limit of which is about 200 °C.

Also important in high speed applications is mechanical strength. Finite element analysis of a typical squirrel cage rotating at high speeds (50,000 rpm with an OD of 76mm for the

starter-generator) shows the highest stress to be the hoop stress on the inner diameters of the end rings. A yield strength of 275 MPa or higher is therefore required of the cage material, as is a high stress-rupture strength for long-term, high temperature operation.

Finally, the cage needs to connect to the magnetic core. The cage must also be a continuous piece. While the cage is composed of conducting bars and end rings, it really acts as if it were one integral piece, at least as far as electrical conductivity is concerned. In other words, if the copper bars and end rings are made as separate pieces, they must be joined so that there is no electrical contact resistance where they meet. In conventional practice, where the aluminum cage is cast in place, this is not an issue since the squirrel cage is formed as an integral piece directly from the melt. If a casting process is not used, however, conductivity will be a concern.

3.5.2 Materials Possibilities

The high electrical conductivity requirement narrows the field of possible cage materials considerably. As described in Chapter Two, only aluminum and copper alloys have conductivities over 60% IACS at room temperature. Even the best rotor class of aluminum alloys is too low in conductivity for high power density applications. Commercially pure electrolytic tough pitch copper has an electrical conductivity of 100% IACS but is too weak to meet the strength requirement. Some silver solders also have high conductivities (about 70%) but again are too weak for a motor [12].

A few copper alloys have both the strength and the conductivity at the necessary higher temperatures. One is Glidcop. Glidcop's strongest grade has a conductivity of 78% IACS and a yield strength of 503 MPa. Other copper alloys that have been used in similar applications are

chromium-copper and zirconium-copper. The latter does not quite have the strength required. Chromium copper, however, has a conductivity of 85% IACS and, properly heat treated and worked, yield strengths over 500 MPa [13]. The properties of chromium copper fall off with temperature at the same rate as those of Glidcop. At temperatures in the 400-500 °C range, however, there is a sharp drop-off in the strength of Cr-Cu due to the precipitation of too much chromium [13]. In the range of operation of the induction motor (<200 °C), however, the properties of Cr-Cu are comparable to those of Glidcop.

Drawn stock of Glidcop is around $17/lb while similar stock of Cr-Cu is around $3.50/lb. These are November, 1995 prices as obtained from SCM Metal Products, the manufacturer of Glidcop, and the Cadi Company, a supplier of copper alloys. For the discussion of possible processes, both Glidcop and Cr-Cu will be considered.

3.5.3 Manufacturing Process Possibilities

There is a close coupling between the manufacturing and the assembly of the squirrel cage. The conventional casting of the aluminum bars directly into the squirrel cage both produces the net shapes of the bars and assembles them into the rotor in one step. Thus, each possibility discussed will include both manufacturing and assembly.

The first option is to mimic the conventional aluminum process by simply substituting chromium copper for aluminum. The problems with this idea relate mostly to the very high melting temperature of the copper alloy (1076 °C) [14]. The copper is being cast into a mold which is the rotor core itself. The magnetic properties of most core materials are damaged when the material temperature rises above about 750 °C. Therefore, since the mold cannot be pre-

heated to a very high temperature, the copper will tend to have many voids inside the slots of the core. It will also damage the rotor core material locally as it cools. Even so, THT Presses does have a patented process for casting copper bars into the rotor slots. However, according to other motor manufacturers, the process is still quite unreliable. Of sixteen rotors tried at Westinghouse Corporation, four were completely unusable because of voids in the slots due to premature freezing, while four more showed degraded performance (Marilyn Short, personal communication, August, 1995).

Another possibility is to fill the slots with the Glidcop powder, press them to achieve full density, and sinter them in place. This would be similar in its effects to the casting technique. The problems with this possibility relate to the high sintering temperature of Glidcop ($T_s \cong 1000$ °C) and the fixturing and post machining operations necessary afterwards [15]. As in the case of casting, the high temperatures involved would damage the magnetic properties of most core materials. Solid Aermet rotors, however, would be unharmed since the heat treatment cycle for Aermet already involves temperatures higher than that to sinter Glidcop.

A problem with the compaction step also arises. Since the slots are long compared to their cross-sectional dimension (i.e., they have high aspect ratios), they tend to exhibit conductivity and strength gradients along their length after being compacted. However, if the slots in the core were open (as described in section 3.4) 100% theoretical density could be achieved down the entire length of the bars when compacted isostatically.
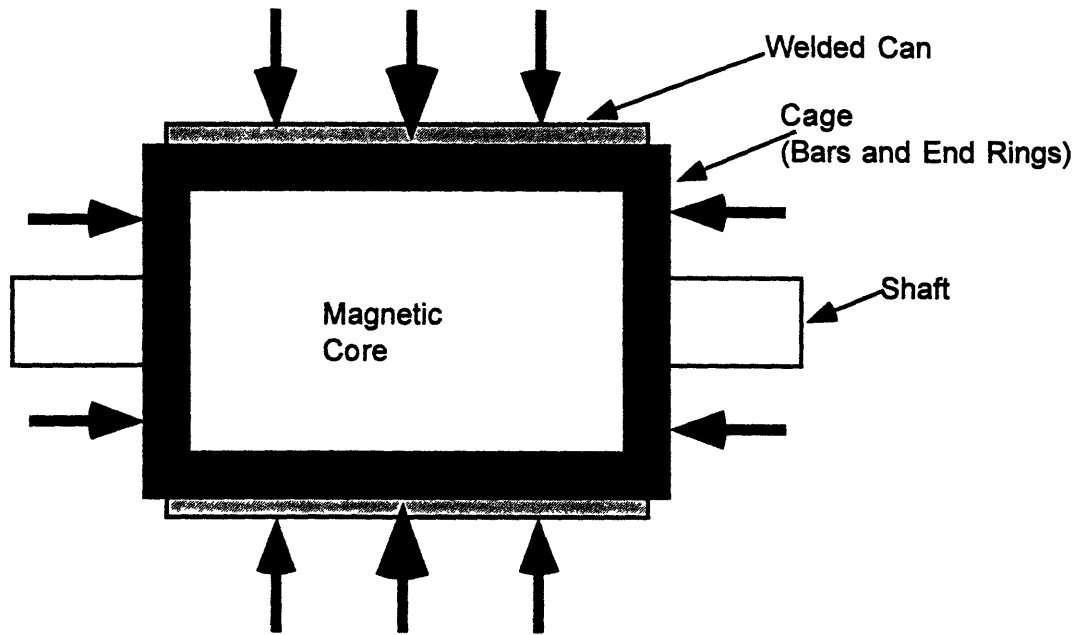
Figure 3.14. Canned assembly (heavy arrows indicate the application of isostatic pressure)

The pressure could be applied isostatically in a HIP (Hot Isostatic Press) unit. The HIP

unit is an inert atmosphere chamber in which the pressure can be raised to upwards of 200 MPa

and the temperatures to over 2000 °C. The HIP process is used mostly in the aerospace industry

to densify and eliminate porosity in large titanium castings [16]. The assembly would have to be

"canned" as in Figure 3.14 to make a powder squirrel cage. Once the process is finished, the can

and the excess powder would have to be machined off. The remaining Glidcop cage would be

sintered to itself and bonded to the Aermet core through diffusion.

Another possibility is to make the bars and end rings in their net-shape first, and then

assemble them to the rotor, rather than attempt to do both at the same time. This is shown in

Figure 3.15. The bars and end rings can be machined, extruded, or drawn. The former is

adequate for very short production runs while the latter methods are more cost effective in larger

quantity.
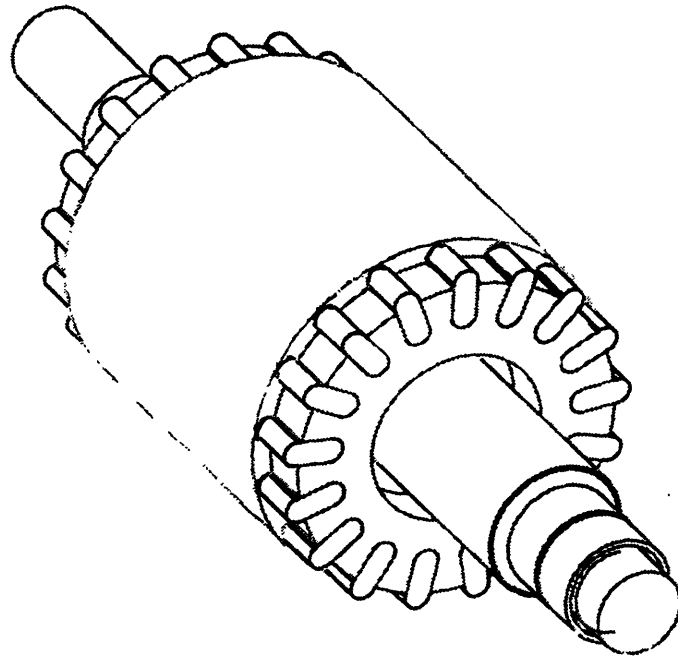
Figure 3.15. Partial assembly showing bars and end rings assembled to a closed-slot core

Several techniques are available to assemble net-shapes to the core. They can be press-fit

and brazed into closed slots in the core. For open slots, however, press-fitting is not possible.

Conventional brazing is not strong enough to retain the bars in their slots under high inertial

loads. Thus, an innovative bonding technique which can form a high-strength joint between the

copper bars and the steel magnetic core, preferably along their entire contact surface is necessary.

The bars and end rings need to have a good electrical connection.

The problem of assembling net-shape bars and end rings into an open slot rotor is solved

using diffusion bonding. The process will be described in Section 3.8.

3.5.4 Squirrel Cage Manufacturing: Conclusions

It was seen in Section 3.4 that an open-slotted, solid Aermet core was the best way of manufacturing the core. Thus, only two materials and two processes remain for the cage construction. The two possible materials are Cr-Cu and Glidcop. Both can be obtained in either drawn or powder form. Both can be used either in the powder form and sintered to the core using the HIP process, or drawn to shape and diffusion bonded to the core. If reliability issues can be resolved, the copper casting process may be useful for machines with lower stresses that can use conventional Si-Fe laminated cores with closed slots.

3.6 The Shaft

3.6.1 Materials Possibilities

Since the high speed motors have relatively low torque (about 34 N-m for the starter/ generator), the primary mechanical requirement of the shaft is accuracy. Accuracy is a result of process and the accuracy required dictates the use of centerless or cylindrical grinding. The accuracy required on the bearing surface of the starter/generator shaft is ±2 μm on the 20 mm diameter [17]. Several steels have the necessary strength for the application. The alloy currently in use by SatCon is 4340 steel.

With the possibility of diffusion bonding or HIP-ing the entire assembly at an elevated temperature, another requirement on the shaft emerges. The heat treatment for the shaft steel must be compatible both with the high temperatures encountered in diffusion bonding and with the heat treatment given to the rest of the assembly (i.e., the core and the cage). Since Aermet is

similar to stainless steel, it is likely that a stainless steel alloy would be heat treatment compatible with it.

There are thus three possibilities for shaft material: Aermet, a stainless steel alloy, and 4340. Aermet can be immediately ruled out. The price per pound of Aermet is twice that of either a stainless steel or 4340. Additionally, Aermet is not currently fabricated in standard centerless ground bar stock. Alloy 4340 can be ruled out because of the incompatibility of its heat treatment with the rest of the assembly. The alloy chosen is 410 stainless steel. This alloy has virtually the same strength as the currently used 4340 at almost the same cost. In addition, with proper heat treatment, the hardness of 410 can be increased above that of 4340, which is good for the bearing surfaces.

3.6.2 Assembly with the Core

Conventionally, core assembly is with keys or splines. For a high speed motor, assembly is complicated by the high stresses and thermal loads encountered by the core. Currently, SatCon assembles its shafts in one of two ways. One method is a shrink fit between the shaft and the core. This is a labor intensive assembly process requiring tightly machined components ($\pm$ 6 μm on a 30 mm diameter). Another method used is the machining of integral shaft/cores. This is very costly in terms of machining time and wasted material.

Other ways to assemble the shaft and core include HIP-ing, CIP-ing (cold isostatic pressing) and diffusion bonding. The high temperatures involved in HIP-ing would likely damage the accuracy of the shaft. CIP-ing would use very high pressures (up to 350 MPa) to actually yield the core and the shaft and make their asperities flow into one another. This would

be essentially a microscopic mechanical press fit. An interlayer of material that easily diffuses into each material (e.g., nickel or a nickel alloy) would have to be placed between the shaft and the core to form a diffusion bond [18].

3.6.3 Shaft Manufacturing: Conclusions

The most accurate shaft would be centerless ground bar stock of 410 stainless. To maintain this accuracy, the shaft could not undergo the high temperatures of a HIP process. The CIP process is a possibility if the high pressure does not affect the accuracy of the shaft. This leaves either mechanical fitting (shrink fit) or lower temperature diffusion bonding. Lower temperature diffusion bonding depends on finding a suitable interlayer that will diffuse into both materials to create a bond without the application of excessive temperatures and pressures.

3.7 Impeller Caps
3.7.1 Material Possibilities

The same considerations of heat treatment compatibility hold for the impellers as for the shaft. Since the whole assembly may be bonded and heat treated together, the materials must be compatible. The impellers also have a strength requirement (about 550 MPa yield minimum) that is satisfied by 410 stainless. Thus it is the material of choice.

3.7.2 Process Possibilities

The parts can either be made using a casting or a powder metallurgy process. Using PM generally involves the added cost of manufacturing the powder, not present for castings. In

addition, as with the core, the cross sectional area of the impeller caps is rather large (a 89 mm OD) requiring a large press capacity. PM would be competitive in terms of the accuracy of the part, but in this case only the ID of the impeller lip needs to be particularly accurate.

The accuracy on this dimension results from the need to either press fit or diffusion bond the impeller to the end ring. The accuracy required for a press fit is +0.00, -0.04mm. The accuracy for a diffusion bond between the end ring and impeller is substantially relaxed because Cr-Cu has a 50% larger coefficient of thermal expansion than 410 stainless [13]. The blades of the impeller need not be held to very tight tolerances. So the process of choice is a casting process, probably investment casting.

3.8 Rotor Assembly Using Diffusion Bonding

SatCon's assembly of a copper squirrel cage is accomplished mechanically using press and shrink fits. Some brazing/soldering is also used in the SatCon technique of cage assembly, but this is more for continuity of electrical conductivity than for mechanical integrity. This reliance on mechanical assembly has increased cost due to ubiquitously tight tolerances on parts and long and difficult assembly.

It has also been shown that the most cost-effective means of fabricating the magnetic core, which is the highest cost item in the rotor assembly, is to cast it with open slots (the numerical cost comparison is shown in Chapter Four). Open slots present an assembly problem. Brazes and solders for the Aermet/Cr-Cu system are not strong enough to retain the bars under the influence of high inertial loads.

A finite element analysis (FEA) was performed using the ANSYS analysis program [19] to determine the necessary bond strength to retain the squirrel cage on the rotating core. The machine geometry used for the analysis was the starter/generator geometry at its design rotational speed of 50,000 rpm. The dimensions of the open slot shape were taken from the numerical results of the Matlab code (see Section 3.4.3) as being the optimal values. Three dimensional elements were used to analyze a radial slice of the rotor. The slot shape used in the FEA with its dimensions and locations of maximum stresses is shown in Figure 3.16.
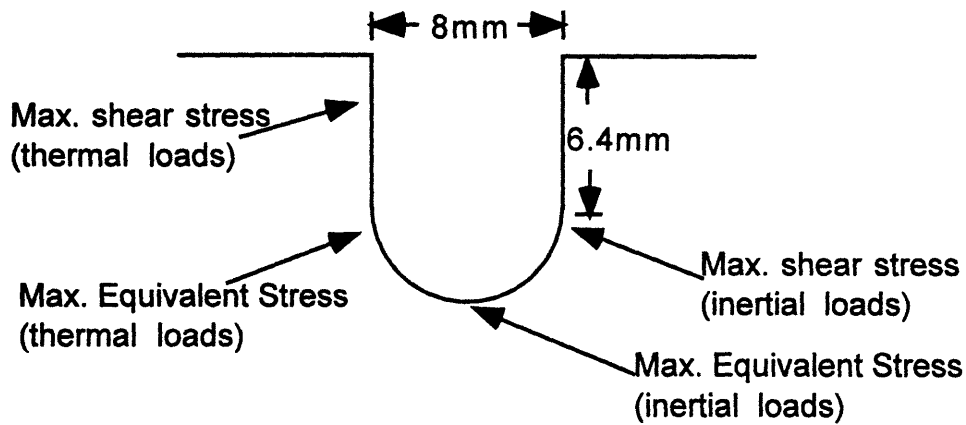
Figure 3.16. Slot shape used in the FEA with maximum thermal and inertial stress locations shown

It was found that the Von Mises equivalent stress at the interface due to inertial loads approached its maximum of 180 MPa at the bottom of the slot radius. The shear stress on the interface had a maximum at the beginning of the curvature of the slot of 13 MPa. Stresses due to differential thermal expansion between the Cr-Cu and the Aermet were calculated separately for a temperature rise of 60 °C. The maximum thermal stress of 172 MPa was found at the

beginning of the curvature of the slot. Maximum shear due to thermal differences was 24 MPa at the top of the slot. Complete results of the FEA are given in Appendix A.

Diffusion bonding has the capability, under the proper conditions, of forming a bond at least equal to the strength of the base metals. As shown by the FEA, this sort of bond (with strength ~350 MPa) will be sufficient to solve the problem of cage assembly. In addition, the Cr-Cu will bond with itself at the interfaces of the bars and end rings, thus providing conductivity continuity. Finally, under the influence of high pressures and temperatures, metal deformation will correct some amount of geometric mismatch between components, thus enabling tolerances to be relaxed.
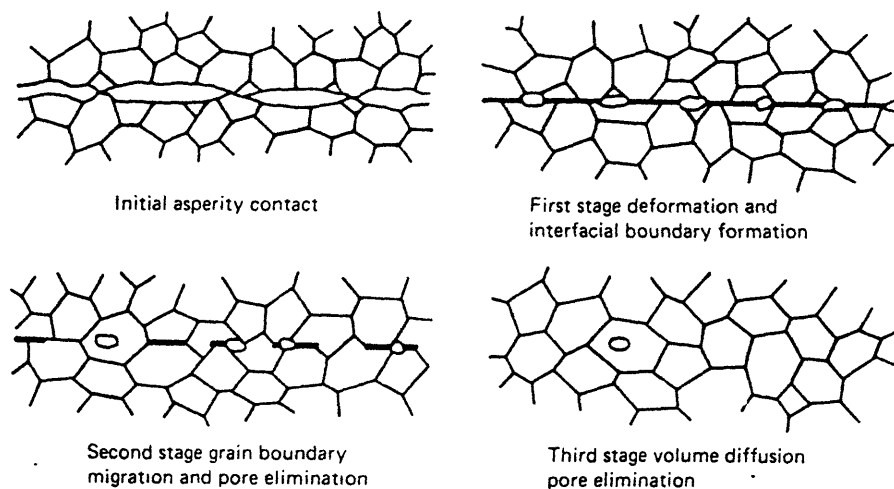
Figure 3.17. Schematic of the diffusion bonding process [20]

The basic mechanism of diffusion bonding is shown in Fig. 3.17. This does not include the presence of an interlayer, which will be necessary for the Aermet/Cr-Cu system in question. The process using a fusible interlayer is shown in Fig. 3.18. An interlayer is necessary for this system because copper and iron have low solubility with each other. Thus diffusion will only

take place slowly and at very high temperatures and pressures. In order to reduce the necessary

pressures and temperatures (and therefore lower cost) a layer of material which diffuses easily

into both metals is used. The material chosen is a Ni - 12wt% P alloy with a relatively low

melting temperature (900 °C). Nickel is soluble in both iron and copper and has a coefficient of

thermal expansion about halfway between the two, thus easing stresses in the bond due to

thermal expansion mismatch [21]. The coefficients of thermal expansion are 10.3, 13, and

17.6 $x10^{-6}$/°C for Aermet [22], Ni-P [13] and Cr-Cu [13], respectively. The Ni-Fe, Cu-Fe, and

Cu-Ni phase diagrams are shown in Appendix B.
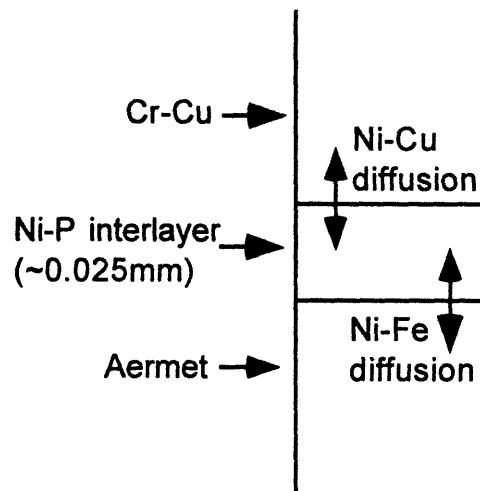
3.18. Diffusion bonding using a fusible interlayer in the Cr-Cu/Aermet system

There are six parameters that affect the bond quality of a diffusion bond:

- temperature,
- pressure,
- time,
- surface roughness,
- surface treatment, and
- interlayer material/thickness.

Elevated temperature is the main variable to increase the rate of diffusion. For diffusion to take place, the atoms of the diffusing media must have enough energy to overcome the potential barrier between sites. The quantity of diffusing material, q, is proportional to the concentration gradient of the material. The constant of proportionality is called the diffusion coefficient:

$$q = D \frac{dc}{dx} \qquad (3.4)$$

where, one dimensionally, $\frac{dc}{dx}$ is the concentration gradient. Equation 3.4 serves to define the diffusion coefficient, D, which increases exponentially with temperature:

$$D = D_o e^{(-Q/RT)} \qquad (3.5)$$

In a physical system, the activation energy, Q, has several values depending on the mechanism of diffusion. Mechanisms encountered in this context include self-diffusion, atom exchange, interstitial motion, and motion of vacancies. The motion of vacancies typically has the lowest activation energy for metals and substitutional/ interstitial alloys and is hence the dominant mechanism. Diffusion bonds are usually created at temperatures around $0.6T_m$ to $0.8T_m$, where T_m is the absolute melting temperature of the most fusible metal in the system [23]. For the purposes of the diffusion bonding experiments on the Aermet/Cr-Cu system, the temperature is raised to melt the Ni-P interlayer. The temperature used is 930 °C, which is .86 T_m of Cr-Cu.

The diffusion length, x, is the average distance that the diffusing molecule penetrates into the diffusion medium. It is related to the diffusivity and the time-at-temperature by:

$$x = C(Dt)^{1/2} \qquad (3.6)$$

where C is a constant of proportionality. Substituting Equation 3.5 into Equation 3.6, an expression relating diffusion length to time and temperature is obtained:

$$x = C'e^{-\alpha/T}(t)^{1/2}$$ (3.7)

where C' and α are new constants to be empirically determined.

The importance of Equation 3.7 for diffusion bonding lies in the relation of diffusion length to bond strength. Unless the time is so long that substantial grain growth or softening occurs in one of the base metals, the optimum diffusion length for a good bond has been found for many metal systems to be ~20 μm [23]. Experimentally, then, when a bond of sufficient strength has been made at two different temperature-time pairs, the two constants in Equation 3.7 can be found. Setting the right-hand side of Equation 3.7 to a constant then gives a relationship between temperature and time-at-temperature necessary for the formation of a bond of the desired strength. This reduces the number of experiments to be performed, and aids in finding the optimum bonding parameters.

Three other bonding variables (pressure, surface roughness and surface treatment) are used primarily to increase the metal-to-metal contact area. Pressure is used to crush the asperities on any surface and increase contact area. It also helps break up oxide layers present on the surfaces. For a process which does not use a fusible interlayer, pressures should be on the order of the yield strength of the weakest metal in the system at bonding temperature (e.g., about 35 Mpa for the Aermet/Cr-Cu system). For a process in which the interlayer is melted, pressures need only be high enough for secure contact.

Surface roughness should be as low as possible to reduce asperity height. One should be careful, however, with reducing roughness. Grinding, lapping, or honing with an abrasive

medium are processes that give excellent surface finishes. For diffusion bonding applications, however, the abrasive particles left on the surface can interfere with diffusion. It has been found that semi-finish machining yields the best surface finish for diffusion bonding [23].

Chemical treatments of the mating surfaces eliminate the surface layers present on metals. Most metals have an oxide layer which can be tens of angstroms thick strongly bonded to the surface. Over the oxide layer are usually layers of adsorbed gases, water, grease, and oil. Surfaces can be degreased with chemicals such as acetone, rubbing alcohol, carbon tetrachloride, and various pickling procedures [23]. Each has advantages in removing different surface contaminants. Adsorbed gas layers and oxides can also be removed by vacuum degassing with or without heating.

To demonstrate the feasibility of diffusion bonding, a diffusion bonded tensile specimen of Aermet and Cr-Cu was made and tested at the MIT Hot Press Laboratory.

Two 13 mm rounds were made, one of Aermet and one of Cr-Cu. Both were semi-finish turned on the surfaces to be bonded. The Aermet was sent out to be plated with a 0.025 mm thick coating of electroless Ni-P. The company applying the Ni-P coating degreased the Aermet in a sodium hydroxide solution and electrocleaned the sample before applying the coating. Both the Cr-Cu and the coated Aermet sample were ultrasonically degreased in an acetone bath before being inserted into the hot press chamber.

Once the samples were in the chamber, they were held in place with a hydraulic press at 0.34 MPa. The chamber was then pumped down to 0.01 Pa and left overnight for the samples (and the rest of the facility) to outgas. The temperature was then raised and held at 930 °C for

one hour. Due to the presence of a graphite die which would be harmed by exposure to oxygen at high temperatures, the cooling of the sample was slow.

It took about one hour to reduce the chamber to room temperature, during which time the copper softened substantially. Nevertheless, the tensile test of the sample gave promising results. The softened copper yielded at 240 MPa, while the bond was left unbroken giving this value as a lower bound on bond strength. Based on the results of the FEA, this bond is sufficient to retain the copper bars, though it has yet to be fully optimized.

3.9 Rotor Manufacturing Process: Conclusions

It has been seen that the manufacturing process design has been driven by the changes that needed to be made to the costliest component. The conventional magnetic core, made of stamped, stacked laminations, was seen as too costly in both materials and processing for high performance applications. In order to use a net-shape process effectively, it was necessary to change the geometry of the core to include a solid core and open slots. This in turn dictated a new way of assembling the squirrel cage to the core that did not rely on geometric constraint. The shaft and impeller caps were simpler tasks. The changes in fabrication technology for them simply involved changing from a piece-work process to a batch or bulk process.

3.10 References

[1] Cronin, J.J. (1976). Selecting High Conductivity Copper Alloys for Elevated Temperature Use. Metals Engineering Quarterly, Aug. pp 1-14.
[2] Roark, R.J. (1989). Roark's Formulas for Stress and Strain. (6th ed.). New York: McGraw-Hill.
[3] Alloy Data Sheet: Hiperco 50 HS (1995). [Carpenter Steel Division]: Reading, PA, Carpenter Technology Corporation.

[4] Pasquarella, G., & Reichert, K. (1990). Development of Solid Rotors for a High-Speed Induction Machine with Magnetic Bearings. Technical Report. Zurich: Swiss Federal Institute of Technology.

[5] Kirtley, J.L. (1994). MatLab script: Polyphase Motor Design Program MOTOR. Massachusetts Institute of Technology, Cambridge.

[6] Sawhney, A.K. (1992). A Course in Electrical Machine Design. Delhi: Dhanpat Rai and Sons.

[7] Kirtley, J.L. (1995). Unpublished Lecture Notes: Mathematically Assisted Design of Electric Machines. Massachusetts Institute of Technology, Cambridge.

[8] Kalpakjian, Serope. (1995). Manufacturing Engineering and Technology. Reading, MA: Addison-Wesley.

[9] Novotny, P. & Maguire, M. Navy Fighter Demands Evolve into Tough Castings. Foundry Management and Technology, Dec. pp.33-36.

[10] O'Handley, R.C. (1996). Unpublished Lecture Notes: Magnetic Materials. Massachusetts Institute of Technology, Cambridge.

[11] Keystone Powder Metal Parts & Self-Lube Bearings (1994). [Keystone Carbon Company]: St. Marys, PA. Keystone Carbon Company.

[12] Brazing Handbook, 4th ed. (1991). Miami: American Welding Society.

[13] ASM Handbook, Vol. 2: Non-ferrous Materials: Properties and Materials Selection Guide. (1995). Materials Park, OH: ASM International.

[14] Chakrabarti, D.J., & Laughlin, D.E. (1984). The Cr-Cu (Chromium-Copper) System. Bulletin of Alloy Phase Diagrams, Vol. 5, No. 1 pp. 59-67.

[15] Glidcop: Copper Dispersion Strengthened with Aluminum Oxide (1994). [SCM Metal Products]: Research Triangle Park, NC. SCM Metal Products.

[16] Lessman, G.G. & Bryant, W.A. (1972). Complex Rotor Fabrication by Hot Isostatic Pressure Welding. Research Supplement, Welding Journal, 51 (12). p. 606-s.

[17] The Torrington Company Service Catalog (1988). [Torrington Company]: Torrington, CT. Ingersoll-Rand.

[18] Schwartz, M. (1967). Modern Metal Joining Techniques. New York: Wiley-Interscience. pp. 370-470.

[19] Swanson Analysis Company. (1995). ANSYS Ver. 5.2. Milford, OH: Swanson Analysis Company.

[20] Welding Handbook, 8th ed. (1987). Miami: American Welding Society.

[21] Ishida, Yoichi (ed.). (1987). Fundamentals of Diffusion Bonding. Amsterdam: Elsevier. pp. 71-88.

[22] Alloy Data Sheet: Aermet 100 (1995). [Carpenter Steel Division]: Reading, PA. Carpenter Technology Corporation.

[23] Kazakov, N.F.(ed.). (1985). Diffusion Bonding of Materials. Oxford: Pergamon Press, pp. 10-70, 162-166, 201-210.

Chapter 4:

COST ESTIMATES

4.1 Introduction

Designing for cost requires accurate cost estimates, at least relative ones, across various processes. Making a cost estimate of a machining process is a fairly easy task. Material removal rates for various processes and materials are well known, the cost per pound of a material can be easily obtained, and the price per hour of machining time can be obtained from any job shop. This information, along with a working drawing of the part, enables a quick calculation of machining cost. For other processes, however, the method of estimation is more complicated and usually a vendor must be consulted. This can be difficult in the early stages of design, without a final drawing to send out for quotation. The vendor's quotation will also depend on projected volume and required delivery time.

This chapter will present the cost estimate per rotor for the diffusion bonded assembly process developed in Chapter Three. This cost will be compared to conventional industrial and current SatCon practice. The five main processes to be compared are shown in Table 4.1. The top three rows are current practices as described in Chapter Two. The fourth row is a process using the copper casting technique described in Chapter Three. The bottom row of entries is the new manufacturing process developed in Chapter Three. The costs per rotor listed in the table are for the core and cage material and assembly only, except in the case of industrial practice where only the price per core is listed. The applications column indicates the quality of the result

of the process in terms of how high a stress the fabricated rotor can maintain. This relates

directly to the maximum power density that the motor can develop using that rotor.

All the prices presented in this chapter are from vendor quotations, not all of which could

be printed in this thesis for confidentiality reasons. The quotations which can be printed, which

are mostly related to the costs of the new diffusion bonding process, form Appendix C.

	Core material/process	Cage material/process	Applications	Cost/Rotor (volume)
Conventional Process	stamped Si-Fe	die cast Aluminum	lowest stress	$6.33** (1500+)
SatCon Prototype Processes	machined Aermet	machined/press fit Glidcop	highest stress	$9450 (10)
	hydroblanked Co-Fe	machined/press fit Glidcop	intermediate stress	$4067 (5)
New Possibilities	hydroblanked Co-Fe	die cast Cr-Cu	intermediate stress	$1737 (50+)
	investment cast Aermet	extruded/diffusion bonded Cr-Cu	highest stress	$275 (50+)

Table 4.1. Manufacturing process possibilities compared in this chapter
*   **-indicates price for core only*

Section 4.2 will present the cost estimation for the new process in detail, describing the

vendor quotations obtained and the machining and assembly time estimates made. Section 4.3

will describe the cost drivers of the processes in the top four rows of Table 4.3 and compare them

with the new process.

4.2 Cost Estimate for the New Diffusion Bonded Assembly Process

The cost estimate for the proposed process is from a combination of vendor quotations for

the net shape processes used, machining time calculations for the pre-assembly machining and an

upper-limit estimate for the cost of diffusion bonding. The vendor quotations are for a projected

volume of 200-500 rotors per year. There is no rush put on delivery. The investment casting

vendor, for example, estimates 11 weeks to deliver a sample casting and bulk delivery 9 weeks

after sample approval.

The investment casting quotations for the core and impellers are based on the geometry of

the starter/generator motor. The core drawing features open slots, with slot width based on the

optimum found using the Matlab code (see Chapter Three). The impellers have not been

redesigned for casting, although tolerances have been relaxed. The chromium copper extrusion

quotations are for toroidal end rings and bars of the proper cross section. Using the simple

doughnut shape for the end rings lowered tooling costs for the extrusion since a die was already

available for the necessary dimensions. The tooling cost for extrusion is therefore only the die

for the bars. The shaft is a standard size of centerless ground bar stock.

	Shaft	Core	Impellers	Cage (bars+end rings)
Material	410 Stainless	Aermet 100	410 Stainless	Chromium Copper
Form	Bar Stock	Investment Casting	Investment Casting	Extrusion
Cost/lb (raw matl)	$4.50	$9	$4.50	$3.90
Tooling	----------	$7,000	$11,100	$2,850
Cost/rotor (material + process)	$10.51	$91.40	$24.00	$13.12
Total Cost per Rotor (Pre-Assembly)	$140	Total Tooling Cost (for net-shape processes)		$21,000

Table 4.2. Summary of costs for the initial shapes of the assembly

Table 4.2 summarizes the vendor quotations for the initial shapes of the assembly. The investment casting quotations are for at least 200 units/year and the extrusion quotation is for about 1000 units/year. The shaft, an in-stock standard product, is priced regardless of volume. The extrusion quotation is given in dollars per foot. There are about 1.4 meters of bars per rotor and about 76 mm of end ring per rotor. The costs listed are on a per rotor basis. For example, the impeller price is that for two impellers, since there are two per rotor.

The next part of the cost is the in-house machining and assembly. Labor cost for the simple (virtually automatic) machining and assembly is about $70/hour. Pre-assembly machining consists of three operations. Since the shaft and cage stock is bought in standard lengths (from 3 to 3.6 meters), they must be cut to the proper length. The shaft must also have a machined shoulder for placement in the core.

Assembly consists of placing the core in the can in which it will be diffusion bonded. The can is a stock low carbon steel sleeve, 1.25 mm thick. The bars and end rings are then assembled to the core and the impeller caps act as the top and bottom of the can. The shaft is also inserted. All parts must be degreased before bonding. The bars and end rings must also be plated with electroless Ni-P before bonding. The can must then be vacuum sealed and welded. The cleaning, assembly, sealing, and welding are included in the vendor quotation for diffusion bonding.

Component	Machine	Operation	Fixture	Machine	Total Cost
Shaft	Auto-Feed Lathe	Turning for shoulder	.3 min/shaft	4.1 min	$5.13/rotor
Shaft	Auto-Feed Lathe	Parting	—————	.8 min	$0.93/rotor
Bars	Auto-Feed Vertical Saw	Cut to Length	.5 min/ 17 bars	1.5 min/ 17 bars	$2.33/rotor
End rings	Auto-Feed Vertical Saw	Cut to Length	.05 min/ 2 rings	5.75 min/ 2 rings	$6.77/rotor
			Total Cost per rotor for pre-bonding assembly		$15.16

Table 4.3. Summary of operations and costs of pre-diffusion bonding assembly

Table 4.3 shows the operations to be performed on the shaft and cage stock. The fixturing and machining times are given for quantities that make one rotor so that all costs in the right hand column are on a per rotor basis. For instance, it takes about 3.5 minutes to properly fixture the bar stock in the automatic-feed lathe [1]. A 3 meter length of centerless ground stock gives about 12 shafts, so the fixturing time per shaft (and hence per rotor) is about .3 minutes. The same argument is made for the bar and end ring fixturing and machining times.

Optimum diffusion bonding of this kind of assembly is not currently industrially practiced. The nearest approximation is the HIP process. The pressures and temperatures encountered in the HIP unit are around 150 MPa and 830°C at times of 2-4 hours [2]. These conditions will produce the copper-Aermet diffusion bond required by the induction rotor but are unnecessarily high. Lower pressures (35 MPa or less), comparable or lower temperatures (600-900 °C) and shorter processing times (<1 hour) would allow for the use of less costly apparatus

and could be done in-house by SatCon. Therefore, the quotation from the HIP vendor is considered an upper limit on the diffusion bonding process until optimum parameters for the diffusion bond are found. The vendor quotation for 1000 rotors is $105/rotor. This includes assembly, welding, vacuum sealing, and the actual HIP process. After the bonding, the low carbon steel can in which the assembly has been placed must be turned off before heat treatment and final grind. The turning procedure will take approximately 5.9 min to fixture and machine, adding another $6.90 per rotor to the total cost.

The assembly will again need to be heat treated after bonding. Since the cycle for the assembly (solution treat, quench, aging) is similar to that for other metals the assembly can be treated with other parts. Vendor quotations indicate the cost of vacuum heat treatment to be about $0.85/lb of material in quantity, bringing heat treatment to about $8.50/rotor. For heat treatment, unless quantities are large, the difference in cost between a custom heat treatment and one that can go with other parts is sizable. Many vendors would not quotation the induction rotor assembly in quantities less than 1000/year if it had a heat treatment cycle unlike anything else. Standardization is key to reducing cost.

The last step of the process is the finish grind on the OD of the shaft and the core. Since this is the necessary last step and is the same for any rotor, it does not affect relative processing costs so it is not included.

Table 4.4 summarizes the cost per rotor of the induction motor rotor using the new process. It is a conservative estimate for volumes of 500-1000 units per year. The next section will summarize the costs involved in two fabricating processes currently in use by SatCon: using

hydroblanking to make a laminated Co-Fe core with machined copper bars, and machining a solid rotor from Aermet. The new process will be shown to result in a substantial cost savings.

	Item	Cost/ Rotor
Net shapes	Shaft	$10.51
	Core	$91.40
	Impellers	$24.00
	Cage	$13.12
Processing	Pre-assembly machining	$15.16
	Assembly and bonding	$105.00
	Post-bonding machining	$6.90
	Vacuum heat treatment	$8.50
	Total Cost per rotor	$275.00

Table 4.4. Summary of the cost per rotor estimate for the new process

4.3 Cost Comparison with Other Processes

For intermediate stress applications like the starter/generator, laminated stacks of the higher saturation flux density Co-Fe alloys are used. The prototype starter/generator laminations were hydroblanked, a proprietary process of Wingard & Co. involving rapid blanking with a hydraulic press. The hydroblanking tooling, including fixture and die, cost $7627. The laminations, for quantities enough to make six rotors, were $3.08/lamination. Stacking and welding for the core was another $888.34/rotor in a quantity of three rotors. This brings the total

cost of a hydroblanked core to $1597/rotor (given that there are about 230 laminations per rotor) plus $7627 for tooling. This figure is for very low quantities and would likely decrease as volume increases.

It is instructive to compare this to the cost of fifty cast Aermet rotors. The investment casting quotation cites a price of $60/rotor for quantities of 50 rotors plus $7000 tooling cost. The investment casting quotation does not include the material cost of Aermet (it normally would but the vendor does not normally cast Aermet and thus does not have it in stock) so another $41.40 must be added. Thus the price of 50 cast Aermet rotors, including tooling, is $12,070 while the price of three hydroblanked Co-Fe rotors is $12,418.

The quality of the product must also be considered. The Co-Fe rotor is manufactured to much tighter tolerances than the Aermet, but if the assembly is diffusion bonded rather than mechanically press fit, these tighter tolerances are unnecessary. Both materials have similar hysteresis losses, but the Aermet is solid rather than laminated so losses will be higher. The Co-Fe has higher permeability, resulting in higher efficiency at a given size and speed. On the other hand, Aermet can be run at much higher speeds and larger diameters due to its substantially higher strength even in the as-cast condition. The trade-offs are equivocal, but the cost differential is undeniable.

A more direct comparison can be made between the new process and the machined Aermet turbine alternator rotors. The low-speed (60,000 rpm) rotor is comparable in size and shape to the starter/generator geometry used to generate the cost estimate for the new process. It was machined as an integral shaft/core, rough machining of which cost $700 per rotor due to the hardness of Aermet and the enormous amount of material removed. Further detail to the rotor

81

was added in intermediate machining, which cost $1125. Much of the detail during this stage, however, was added to the couplings on the ends of the shaft and therefore should be discounted for the sake of comparison. The closed slots of the rotor were made using the EDM process due to the length of the core (about 12.7 cm) and the tight tolerances required by shrink-fit assembly. The EDM process cost $1140 for the start holes to insert the wire to cut the slots. The actual wire-EDM of the slots cost $4750, of which $3000 is a tooling charge, so the cost per rotor is $1750. There are 38 slots in this rotor. This does not include the cost of Aermet, and the waste generated machining a 3.8 cm diameter shaft out of a 11.4 cm round billet for a length of around 17.7 cm.

Moving from the core to the copper bars, it has already been noted that Glidcop is around $17/lb while Cr-Cu is $3.50/lb (both depend on the price of copper at the time of purchase). Conventionally machining the copper bars for the starter/generator cost $65/bar, bringing the 17 bars necessary for the motor to $2470 (almost the price of the extrusion die). It was necessary to EDM the Glidcop bars of the low speed alternator because of a 0.4 mm thermal expansion stress-relief groove running down their lengths. This raised the price of these bars to $205 per bar. Such a groove would be unnecessary with open slots.

If for some application the improved performance of a Co-Fe laminated core were worth the increased core cost, would diffusion bonding extruded shapes still be the best way to accomplish cage assembly? The cost of machining Glidcop bars has already been given, and the cost to machine Cr-Cu bars is similar. The other two viable options are casting a Cr-Cu squirrel cage with the proprietary die casting process or diffusion bonding. As has been shown, diffusion bonding would cost $13.12/rotor for the raw shapes, $9.10/rotor to cut to length, and

$105.00/rotor to bond. This gives a total of $127.22/rotor plus $2850 for the bar extrusion die for quantities around 500 rotors. The quotation for the copper casting process gives a per rotor price of $140 for quantities of around 200 rotors, plus $20,000 for the die casting mold. Even adjusting the price of the casting process for volume, the processes are comparable. Recall that the diffusion bonding price is high, being based on a HIP quotation rather than the optimal diffusion bonding process. Additionally, there are serious quality issues with the casting process (see Section 3.5.3), namely inclusions in the bars and possible high-temperature induced damage to the core metal. Co-Fe laminations are especially sensitive to improper heat treatment.

The new process is designed to lower the cost of manufacturing a moderate volume of high performance motors and does not try to compete with the production of high-volume, low performance industrial motors. Nevertheless, for the sake of completeness, it is instructive to see what the real costs are of a mature industrial process. Tempel Steel is a major manufacturer of standard, Si-Fe motor lamination stacks. A die for a new motor design costs around $80,000 for a single row stacking die, and $210,000 for a three row indexing die. The single row die makes one lamination stack at a time, and stacks the laminations straight on top of one another, allowing for no skew in the rotor slots. The three row indexing die makes three stacks at a time and has the capability to rotate the laminations to produce skewed slots. Each die is capable of making approximately 500,000,000 laminations during its lifetime, with occasional sharpening.

To punch a 24 gauge (0.63 mm) lamination with the cross sectional area of the starter/generator core costs 4.8 *cents* per lamination on a three row indexing die. The minimum order is 200,000 laminations. This translates into roughly 1515 starter/generator cores. There would be about 132 24 gauge laminations in a starter/generator core making the cost of a core per

rotor about $6.33. The cost per core per rotor for the Aermet casting was $91.40. The industrially produced core, of course, cannot perform like the Aermet.

4.4 Cost Estimate: Conclusions

Clearly, the use of casting greatly reduces the cost of the magnetic core. Without the ability to diffusion bond the cage to open slots, however, casting cannot be employed. This is a good example of the coupling between processes that can greatly reduce (or increase) cost. Another problem solved by open slots that has been shown to reduce cost is the elimination of the stress-relief groove in the copper bars. Due to the vast (50%) difference in thermal expansions between copper and Aermet, grooves were put in the bars which could only be manufactured by EDM, a very costly process. Open slots eliminated the need for grooves, allowing for the use of a bulk net shape process like extrusion.

The cost drivers in the new process are the magnetic core and the diffusion bonding step. Little can be done about the cost of the core, but the diffusion bonding need not be so costly. Lower pressures and temperatures for shorter periods of time should be able to produce an adequate bond with the necessary strength.

4.5 References

[1] Machining Data Handbook 3d ed. (1980). Cincinnati: Machinability Data Center.
[2] Lessman, G.G. & Bryant, W.A. (1972). Complex Rotor Fabrication by Hot Isostatic Pressure Welding. Research Supplement, Welding Journal, 51 (12). 606-s.

Chapter 5

THE GENERAL MANUFACTURING PROCESS DESIGN

5.1 Introduction

This chapter will apply the lessons learned in designing the induction rotor process to

arrive at a proposed systematic approach to this sort of problem. The problem can be stated as

follows:

"Given an assembly, find the most cost effective process by which to manufacture it."

The word that makes this difficult is "most," implying an optimum. It is easy to come up

with *a* process, but how does one know that the optimal, lowest cost process for the performance

desired has been reached? There is an enormous number of manufacturing technologies which

can be used to fabricate each part in an assembly.

Each process has its advantages and drawbacks. For example, a simple, cylindrical brass

bushing could be made using powder compaction, casting, forging, machining, or any one of

several other processes. The cast bushing would probably be the least expensive, while the

machined bushing could be made to the tightest tolerances. The powder metal bushing would be

more expensive than the casting and less accurate than the machined part. During the powder

compaction process, however, the bushing could be oil impregnated and thus self-lubricating in

service.

These processes can couple with one another across different parts in an assembly:

geometric changes to one part to make it compatible for a given process affect the design of other

parts. For example, the cast brass bushing could be made with greater lengths and cross-sectional thicknesses than a powder metal brass bushing. This could affect the design of the bushing's housing, and it could change the load capacity or the moment-bearing capability of the bushing. The manufacturing process cannot be de-coupled from the performance and geometry characteristics of the manufactured part. There has to be a way to ensure that all possibilities have been considered both for each part and for the assembly as a whole.

This problem has been studied in recent years under the name of design for manufacturability, or DFM. Several theories, including the design for assembly (DFA) rules of Boothroyd and Dewhurst, axiomatic design rules, and the methods of Taguchi, have addressed this problem with varying degrees of success in different situations [1]. Not all of them formulate the problem as it is formulated above, but most reach similar conclusions.

The specific manufacturing problem which is the topic of this thesis is a little different from most DFM studies. The cases generally seen investigated in the DFM literature use products which are already on the market and are already manufactured with a given method. The design of the product is then corrected using the suggested systematic approach. For example, Boothroyd and Dewhurst demonstrate the utility of their design for assembly methodology by redesigning assemblies ranging from the front suspension of a GM truck to an IBM Pro Printer [2]. After the new manufacturing process to make the redesigned part is demonstrated, the cost of the new process is compared to that of the original. This is how the effectiveness of the general approach is validated.

In the case of the high-performance rotor for the induction motor, however, the product is new and not currently manufactured in volume. Similar products are made (i.e., low

performance conventional rotors) but the stamping, stacking, and casting processes used to manufacture them are incapable of manufacturing the high performance model. Only prototypes of the product had been fabricated prior to the design for manufacturability. During development the cost of these prototypes was not of great concern. Thus the choice of a manufacturing sequence, both for each part and for the whole assembly, has no *direct* comparison to a previous sequence used to manufacture the same product, as most DFM studies do.

The process to be introduced is similar to other DFM analyses, but from the perspective of a manufacturing engineer with a new product and only a prototype. In general outline, the process is as follows:

- Define the problem
    - in terms of the machine's function and modeling
    - in terms of expected production volume
- Divide the assembly into parts or groups of parts with the same function ("functional decomposition")
    - identify cost drivers and crucial dimensions
    - eliminate unnecessary duplications of function
- List fabrication and materials possibilities for each part
    - ensure that all available technologies are considered
    - do rough DFF (design for fabrication) for each technology
    - obtain cost estimate for each feasible process
- Create production sequences for the whole assembly
    - analyze the couplings between parts and processes
    - choose lowest cost sequence

5.2 Problem Definition

The first step in designing a manufacturing process is to develop an understanding of the operation of the part or assembly in question. The relationship between geometry, material properties, and part performance should be known and, if possible, mathematically modeled. For

the induction machine, Section 1.3 gave an overview of how induction motors work and how their performance is modeled. A Matlab code analyzed geometry and material property effects on performance. Additionally, the designer should have a good intuitive feel for how changes wrought by a particular process affect the machine.

While the manufacturing process designer does not have to be a designer of the machine to be manufactured, he should keep an open mind regarding geometry changes which would drastically reduce cost. An example of such a change would be the switch from closed to open slots in the induction motor rotor. Changing the geometry to include open slots allowed for the cost-effective use of investment casting that would not have been possible otherwise. Once it was seen that there was a method to retain the squirrel cage with open slots, a new motor geometry which was previously un-manufacturable became possible. It was then necessary to use the mathematical model to evaluate the effects of open slots on performance.

These sort of design changes are changes at the manufacturing level, after a design has been completed and a prototype built and tested. Ideally, of course, the design of the machine and the design of the manufacturing sequence should be done concurrently. That way, for example, designers would not have spent so much time optimizing slot shapes for closed slots. They would have known that they had the option to use open ones. Concurrent engineering should be practiced but often is not. In this case, it was not.

After understanding the machine, the next most important piece of information regarding manufacturing is expected volume. This is usually given in number of units per year. Again, for an established product that is being re-engineered according to DFM rules, this is an easier number to acquire. For a new product, especially a new product from a new company, this can

be more difficult to estimate. A change in the number of units per year can change the manufacturing landscape drastically. For example, if only ten induction rotors were going to be made per year, it would be more expensive to amortize the cost of tooling (e.g., the investment casting molds and extrusion dies) over those ten units than it would be to machine each one. Once the number of units per year exceeds about 100, however, the net-shape processes described can be used quite effectively.

At the next level in terms of number of units per year, volume will determine whether much of the work is outsourced or done in house. Net shape processes requiring large amounts of capital and expertise (e.g., castings, powder metallurgy) are almost always outsourced. For example, SatCon has no reason to become a foundry doing its own investment castings, nor to run an extruding or powder metallurgy operation, no matter how large volume is. Even automobile manufacturers with volumes in the millions of units per year outsource fabrication processes like investment casting [3].

In the electric machinery industry, the manufacturers of motors typically only do final assembly and finish machining in house. For example, the stamping and stacking of the laminations is outsourced by the company that designed the machine to a company that does stamping and stacking for several motor manufacturers [4]. Similarly, the casting of the aluminum squirrel cage is also done by a firm specializing in pressurized die castings. Operations like the insertion of the shaft and the winding and potting of the motor are done in house.

5.3 Functional Decomposition

After the machine to be manufactured has been modeled and the effect of geometry and material property changes to the assembly can be analyzed, it is very helpful to do a "functional decomposition" of the assembly. This involves breaking the assembly into functional components, parts or groups of parts which have the same function. The function of each component and of the assembly as a whole can then be described. This decomposition helps focus any design effort, not just the design of a manufacturing process, but there are a few points which relate directly to manufacturing. The separation of an assembly into parts or subassemblies with very specific and well-defined functions is even more important when a team effort is involved. Each member of the team then has a specific problem which can be analyzed concurrently with the other parts in the machine. Functional decomposition facilitates concurrent engineering.

The first step of the functional decomposition process involves generating detailed specifications of the machine. This should be done before any design, whether a manufacturing analysis is performed or not. The more cogent point for the manufacturing analysis is the decomposition of the design into components which have the same function and thus can be manufactured by the same method and with the same materials.

The second step is to list each part in the assembly and enumerate its function. Parts with the same function should be grouped. The first thing to ensure is that there are no unnecessary duplications of function across groups. The next is to discover which parts are the most costly so that design effort can be focused there. For example, it was realized early in the design of the

induction motor rotor that the magnetic core was typically the most complex part to manufacture, and contained the most inaccuracies and limitations when fabricated by conventional means. The decomposition should also point out the most important dimensions of the machine, so that accurate and repeatable processes can be used to maintain them.

5.4 Processing and Materials Options

This is the step that requires the most breadth of knowledge on the part of the designer. For each part, the manufacturing engineer must list every possible process and material that could be used to fabricate the part. Even if a fabrication technique would require some redesign of the geometry of the part, it should be listed. This is to ensure that all available fabrication technologies and materials are considered.

The best way to make sure a complete list has been generated is to use a reference book with a good directory of fabrication techniques for various materials, containing descriptions of virtually every commercially available manufacturing process [1]. The most important information here is knowledge of the dimensional tolerances, surface finishes and geometric capabilities of each process.

Another way to stay current on fabrication technologies is to obtain a directory of the local job shops and what they have available. A brochure from, say, a powder metallurgy company usually contains a list of materials they use, several pictures of typical parts produced by the process and simple design guidelines. One of the easiest ways to lower cost is to use commonly available materials, shapes, and processes. In addition, often the only way of

obtaining a cost estimate for a part made by a particular process is to consult the appropriate vendor.

Generally, net shape processes are more cost effective than machining for even moderate production volumes. This is because of reduced scrap (Aermet, for instance is about $10/lb), and reduced labor time in post-processing. As was seen for the rotor and impeller castings, the cost of a simple investment casting mold is relatively low. Since Aermet is very difficult to machine, investment casting lowers cost even at volumes as low as 100 units/year. The same is true of the impellers. For a relatively simple shape which has many repetitive features (17 slots in the core and 15 blades on the impellers), net shape processing pays off quickly.

The process of redesigning a part to make it compatible with a given process is commonly called design for fabrication, or DFF [1]. Normally this simply involves minor geometrical changes like designing generous fillets, calling out tolerances which are achievable by a given process, and avoiding large cross-sectional area changes in a casting. Such changes usually have little effect on the function of the part. In the case of the induction rotor, however, the elimination of a feature which would have caused casting problems introduced severe limitations on how the cage would then be fabricated and assembled to the core. This will become more apparent when production sequences are generated in the next step.

Once a DFF has been done, the cost of the part can be estimated by a vendor. A cost estimate should be obtained for each feasible process for each part for the expected volume.

5.5 Production Flow Charts

Once a list of possibilities for each separate part has been made, the production sequence of the entire assembly can be constructed using various items from each list. This is where the couplings between processes becomes apparent. If one could simply create a list of processes for each part, then choose the least expensive process from each list to create the assembly, the job of optimizing the production sequence would be simple. Since all the parts must be joined, however, the geometric requirements of one fabrication technique constrain the choices of technique for other parts. A good example of such a coupling is that between the magnetic core and the squirrel cage of the induction rotor.

The induction rotor can be made with closed slots by machining. For lower stress applications it can be made by stamping a stacked core. At higher cost and low reliability a casting process can be used. All these options are more costly than fabricating the core with *open* slots using investment casting. The squirrel cage, however, could easily be assembled to a closed-slot core using the high-pressure casting method. This technology is conceivably cheaper than other methods of assembling the cage to the core. So in this case, the core is more expensive but the cage is less so.

The rotor can be made quite cost effectively with open slots using investment casting. Open slots, however, make the copper casting technique impossible to use. Thus, the open slots constrain the cage options to powder metallurgy, requiring isostatic pressure and significant post-machining, and diffusion bonding machined or extruded bars to the slots. In this case, the core is less expensive but the cage is possibly more expensive.

Another important point about the coupling of processes is repeatability. Parts which need to be assembled must, in some way, be geometrically congruent, i.e., they have to fit together. Generally, the more accurate the process the more expensive it is. Machined components can be made orders of magnitude more accurately than castings but at much greater expense. Accuracy defines the ability of the process to obtain the desired dimension. Repeatability means the ability of a process to give the same dimensions for every part, whether those dimensions are the nominal dimensions or not. For example, injection molding is not a very accurate process, especially for intricate parts. It is difficult to predict shrinkage, heat flow, plastic flow, etc. It is very repeatable, however. If the initial temperature and the melt and pressure of the press are kept reasonably constant, the process gives parts with dimensions within 2 μm.

Often for parts in an assembly repeatability is more important than accuracy. Consider the case of a shaft being inserted into a rotor. If the processes producing both the shaft and the rotor are very accurate and repeatable, there will never be any problem assembling them. If neither of the processes are accurate or repeatable, then each shaft and each rotor will have to be measured and secondary machining may need to be done to at least one of them. Each rotor and shaft will be a pair that can only fit each other. However, if the process to make the shaft is very repeatable, then the same operation can be done to each rotor to make it fit. A measurement operation is saved and the machining operation is made repetitive, lowering costs. This is true even if the shaft fabrication technique did not give a very accurate shaft diameter. As long as nothing but assembly considerations dictate a given dimension, the repeatability of a process is more important than its accuracy.

5.6 Conclusions: Manufacturing Process Design

The procedure for designing a manufacturing process presented involves assimilating a tremendous amount of information about the geometric and materials properties capabilities of various fabrication techniques (e.g., casting, forging, powder metallurgy, extrusion, machining, stamping, etc.). The most important steps of the procedure are the final two: the listing of materials and processing options for each part, and the production of manufacturing sequence flow charts. The difficulty in systematizing a general approach to designing a manufacturing process primarily arises from the fact that each manufacturing technique introduces geometric and material property limitations on the part being manufactured. Since the parts must geometrically fit together to form the assembly, there is a coupling between the manufacturing of a part and how it is assembled. The arrangement of the options for each part into various possible manufacturing sequences shows the designer how the processes work together. By systematically considering all options, an optimum can be reached.

5.7 References

[1] Bralla, J.G. (ed.). (1986). Handbook of Product Design for Manufacturing-A Practical Guide for Low-Cost Production. New York: McGraw-Hill.
[2] Boothroyd, G., P. Dewhurst, & W. Knight. (1994). Product Design for Manufacture and Assembly. New York: Marcel Dekker.
[3] Kalpakjian, Serope. (1995). Manufacturing Engineering and Technology. Reading, MA: Addison-Wesley.
[4] Tempel Motor Laminations (1993). [Tempel Steel Services Division]: Niles, IL. Tempel Steel Company.

Chapter 6

CONCLUSION

Polyphase induction motors featuring a squirrel cage rotor were developed around the turn of the century. Their basic geometry, the cage and core materials, and the methods used to fabricate them have changed little since then [1]. Recent advances in power electronics have made high and variable speed induction motors possible and controllable. High speed induction machines have applications in high speed machining, turbomachinery and electric vehicles.

The limitations on the performance of the machines in terms of operating speed and power density are introduced by the materials and the manufacturing methods used. An opportunity for improved performance through improved manufacturing practice exists. However, improved machines will only have market potential if developed at a reasonable cost.

Induction motors and the methods used to manufacture them are examples of very mature technologies. The stamping process used to make the laminations, for instance, has undergone iterations in geometry and materials to the extent that one may say that it has been optimized. The same is true for the stacking, rolling, and die casting technologies used to fabricate the rotor. Improvements to these processes will produce only incremental increases in motor performance. Revolutionary improvement is required to make machines with power densities and speeds orders of magnitude beyond those produced by conventional practice.

The new cast rotor/diffusion bonded squirrel cage process shows promise as a process which can produce high performance induction motors at a competitive cost. Using investment

casting to manufacture the Aermet magnetic core is the most cost-effective means of fabricating the most costly component of the rotor. The problem of retaining the copper bars in the open slots produced by the casting process has been solved by a diffusion bonding joining technique. The use of extruded conducting bars and end rings to form the cage has replaced enormous amounts of machining time. The assembly of the extruded shapes into the open slots of the core has eased assembly. Subsequent diffusion bonding gives the assembly the necessary mechanical integrity. The diffusion bonding of the cage also provides excellent electrical connection from the conducting bars to the end rings, eliminating the need for costly brazing procedures.

The feasibility of diffusion bonding Cr-Cu to Aermet has been demonstrated, although further work needs to be done to optimize the bonding parameters and bonding geometry. Further work should also be done on heat treatment for improved magnetic properties of Aermet. Aermet was originally developed as a high fracture-toughness replacement for 4340 in military aircraft structural applications. Its heat treatment procedure has been optimized for fracture toughness with no regard for magnetic properties [2]. Since it has demonstrated its utility as a high strength magnetic core material, its heat treatment should now be adjusted to optimize magnetic permeability and saturation induction.

The new manufacturing process has been shown to reduce the cost of the rotor substantially. The original price to fabricate a prototype Aermet core/copper squirrel cage rotor was around $10,000. The projected cost using the new process, based on vendor quotes and estimated machining and assembly times, is $275 per rotor for a volume of fifty units per year or more.

The experience of designing this manufacturing sequence has also lead to insights about design for manufacturability. A systematic method has been suggested for creating an optimal manufacturing sequence. The method involves the examination of all the manufacturing process options for each part in an assembly and how each process constrains the geometry of the part. The list of options for a given part is then combined with the lists of options for the rest of the parts in the assembly. A series of manufacturing sequences is generated. The cost of each sequence is generated by adding the costs of each separate process. The cost of each separate process can be determined through vendor quotes or calculations of machining and assembly times. The lowest cost sequence is the optimal one and should be chosen.

A manufacturing process design requires a great breadth of knowledge on the part of the designer. It requires the familiarity of the capabilities of a large number of fabrication techniques. This has been demonstrated using the example of the high performance induction rotor process design. A variety of manufacturing technologies have been considered for each component. Each of these processes (casting, extrusion, powder metallurgy, etc.) has been examined. A manufacturing sequence which represents a large cost savings and performance improvement over current practices has been chosen.

References:

[1] Slemon, G.R., and Straughen, A. (1980). Electric Machines. Reading, Mass: Addison-Wesley.
[2] Novotny, P. & Maguire, M. Navy Fighter Demands Evolve into Tough Castings. Foundry Management and Technology, Dec. pp.33-36.

Appendix A:

FINITE ELEMENT ANALYSIS OF THERMAL AND MECHANICAL STRESSES IN OPEN SLOTS

This analysis determines how strong the diffusion bond between the copper bars and the Aermet core must be to resist inertial loads and loads due to thermal expansion mismatch. The motor geometry and dimensions used are the same as were used for the open slot analysis, namely the starter/generator geometry. The open slot dimensions used are those that were determined to give the optimal motor performance. Thus the width of the slot is 8 mm and the depth of the slot (including semi-circular portion) is 10.35 mm.

The analysis uses a three-dimensional symmetric wedge to model the spinning core with embedded copper bars. The geometry is shown in Figure A.1. The x-axis shown is the axis of the motor and the y-axis is radial. Essentially, the geometry is half a slot and half a tooth which, repeated 17 times, forms the entire rotor. The thickness of the wedge is 2.5 mm. The outer radius of the wedge is 42.6 mm and the inner radius is 15.8 mm. The interface between the copper bar and the Aermet core is modeled by enforcing stress and displacement continuity at the boundary. Both materials' properties are on file in ANSYS and are used in the analysis.

The element used is a tetrahedral solid element (Solid 72). There are 6000 elements in the model shown giving an average element leg dimension (nodal spacing) of 0.75 mm. The mesh was generated using the automesh feature of ANSYS. To determine whether this was adequate, convergence was determined two ways: one case was run with twice the number of

elements, and one case was run using a two-dimensional axisymmetric model. In neither case were the results significantly different than the ones shown.

The first runs simulate only the inertial loads (Figures A.2 through A.5) for the rotor spinning at its design speed of 50,000 rpm. Figure A.2 shows the Von Mises equivalent stresses in the Aermet part of the rotor. Figure A.3 shows the shear stress component only. Figures A.4 and A.5 show the same stresses in the copper bar.

The second set of runs simulates only the thermal loads for an operating temperature of 100 °C (Figures A.6 through A.8). Figure A.6 is the equivalent stress in the combined bar/core system. Figure A.7 is the shear stress component. Figure A.8 is the shear stress due to thermal loads in the copper only.
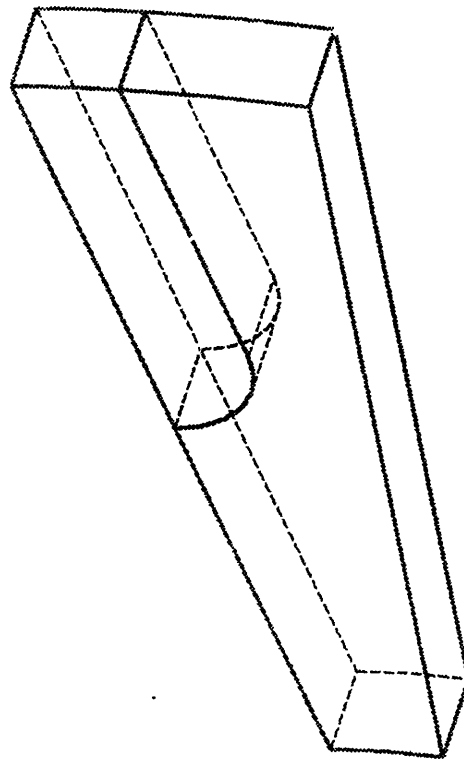
Figure A.1. FEA model geometry showing symmetric rotor wedge and rotor axes
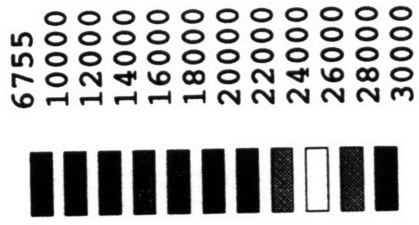
Figure A.2. Von Mises equivalent stresses in the Aermet core due to inertial loading at 50,000 rpm
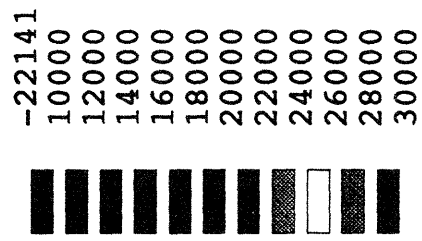
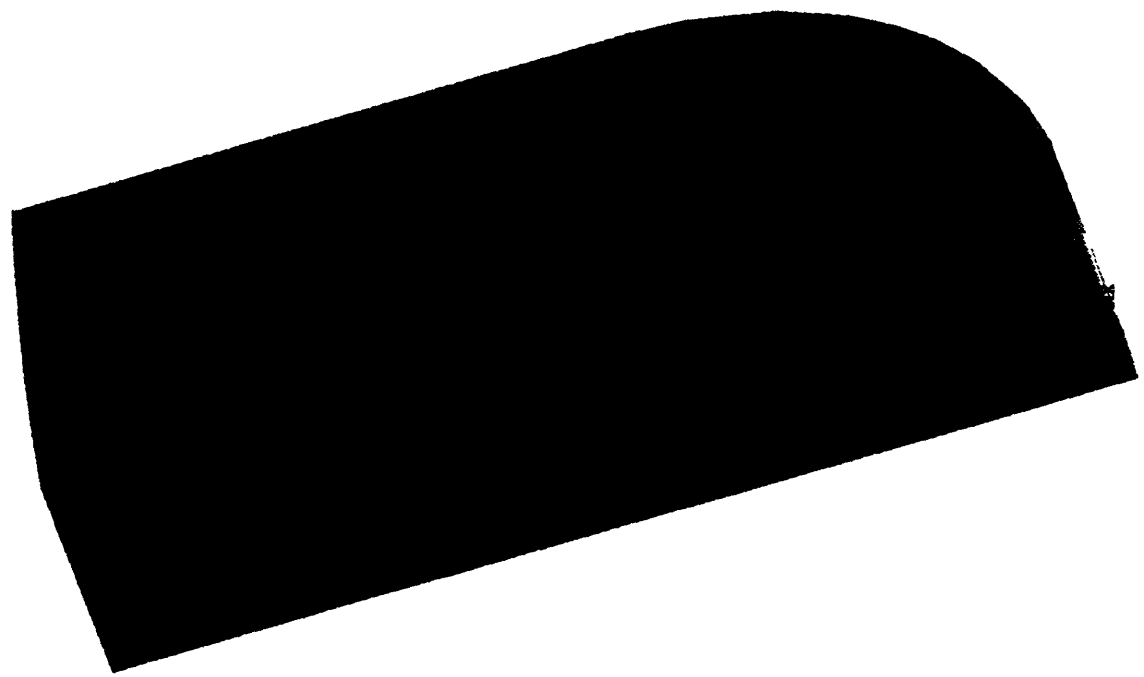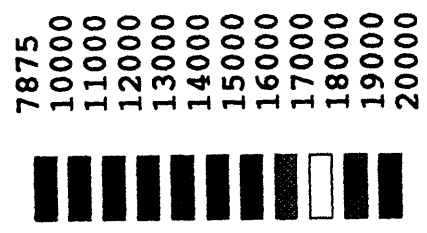*Figure A.3. Shear stress in the Aermet core due to inertial loading at 50,000 rpm*

Figure A.4. *Von Mises equivalent stresses in the Cr-Cu bar due to inertial loading at 50,000 rpm*
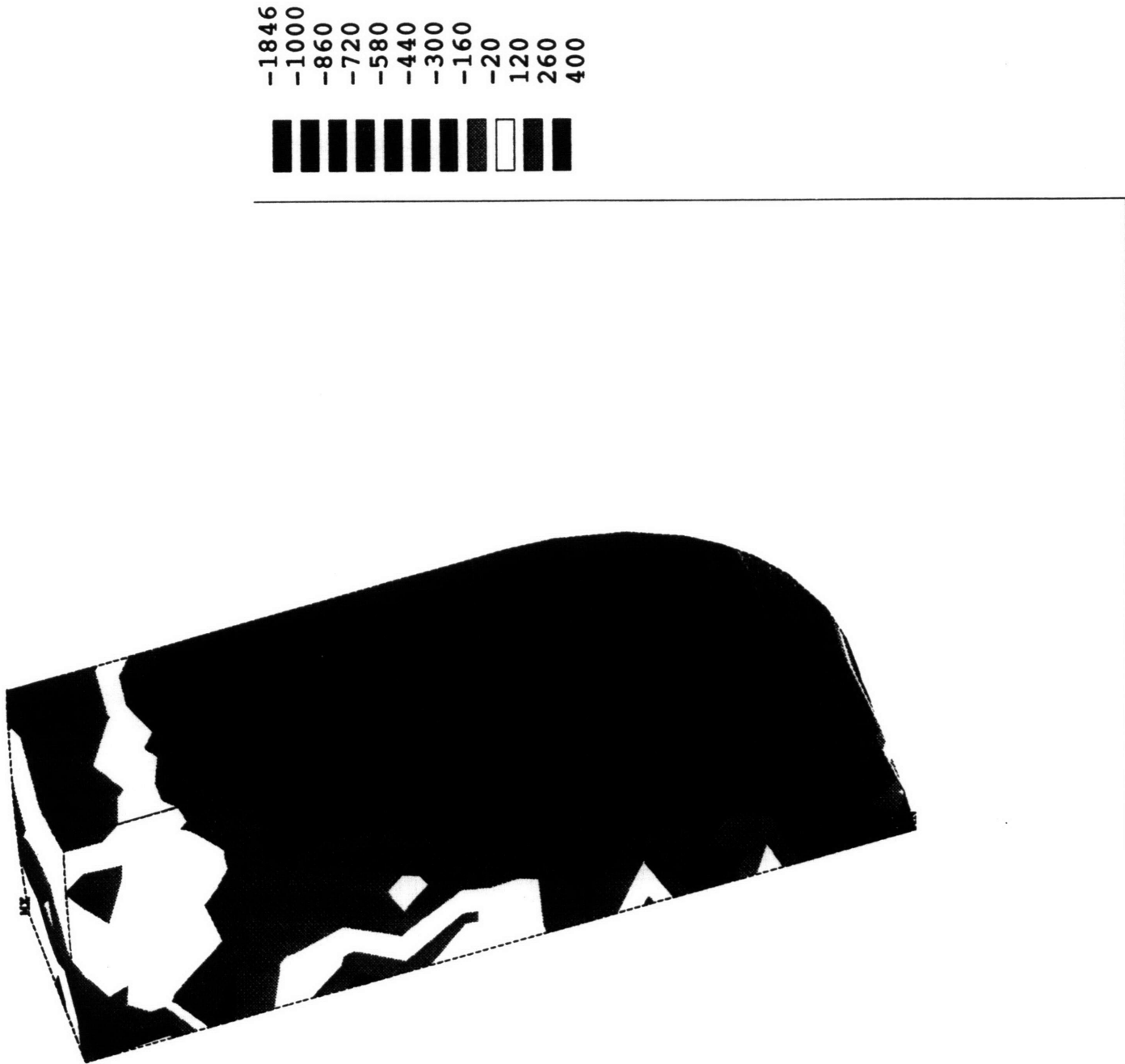
Figure A.5. Shear stresses in the Cr-Cu bar due to inertial loading at 50,000 rpm
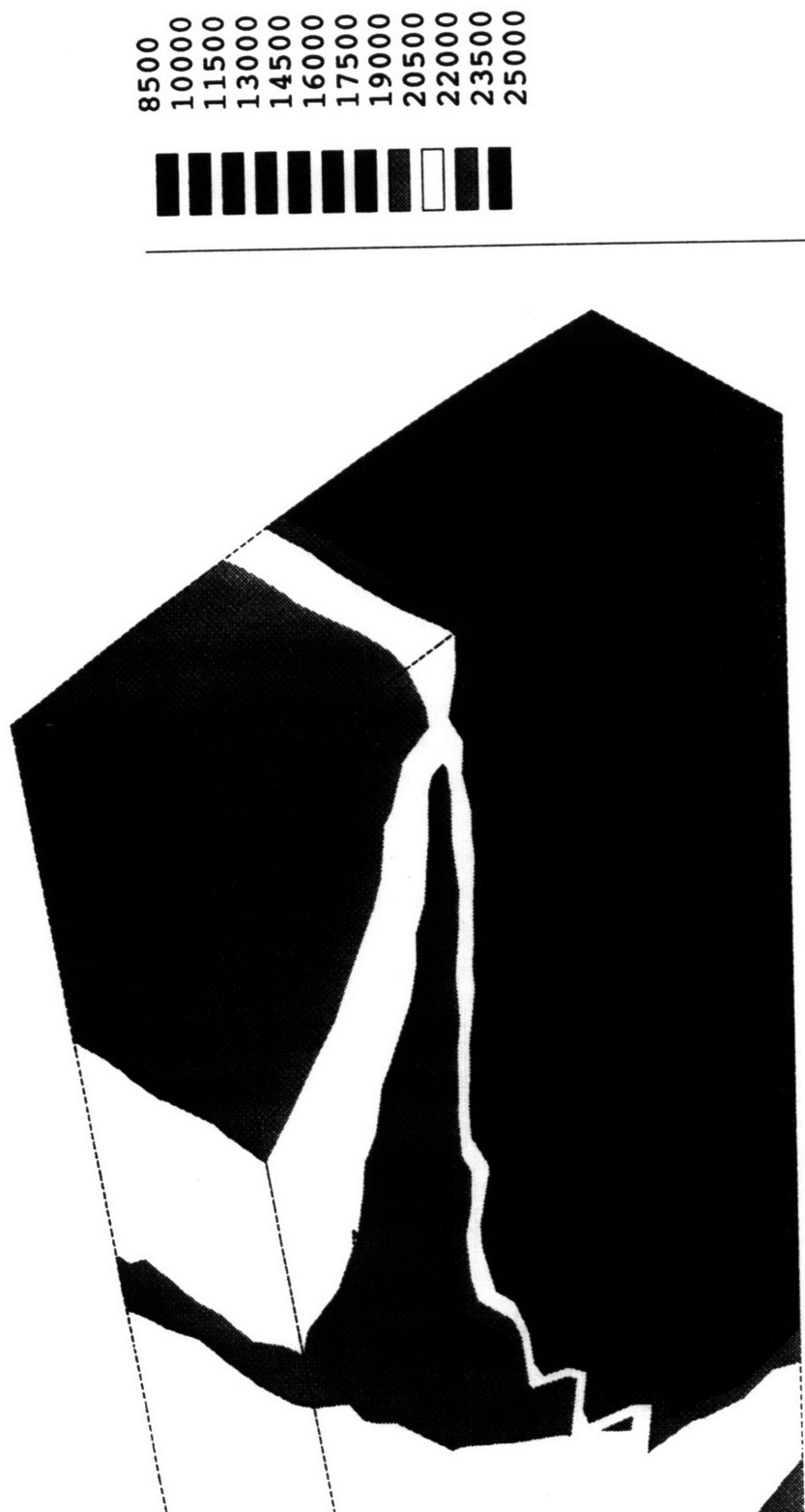
Figure A.6. Von Mises equivalent stresses in the Aermet/Cr-Cu wedge due to mismatched thermal expansion for an operating temperature of 100 °C
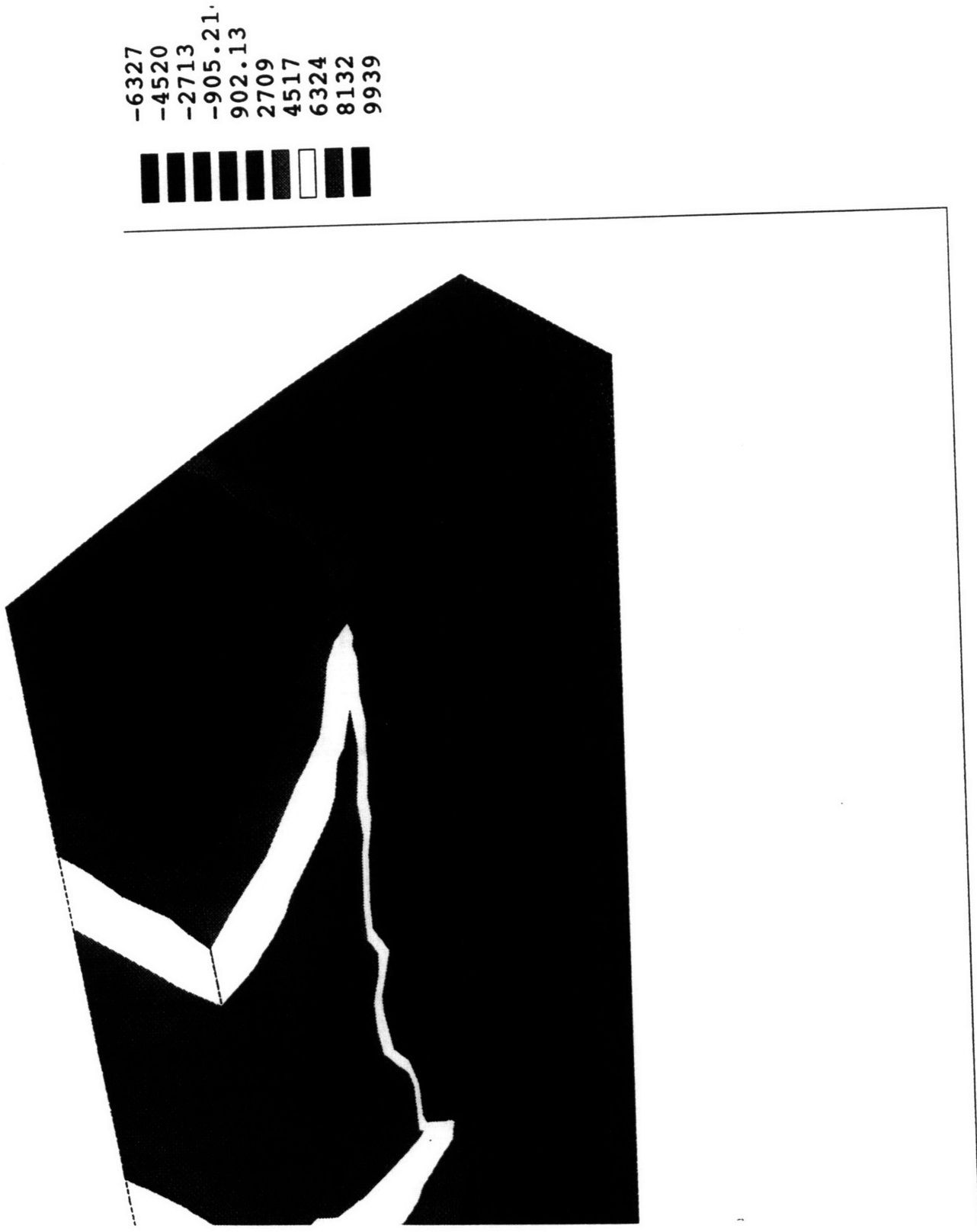
106

*Figure A.7. Shear stresses in the Aermet/Cr-Cu wedge due to mismatched thermal
expansion for an operating temperature of 100 °C*

107

Figure A.8. Shear stresses in the Cr-Cu bar due to mismatched thermal expansion when constrained by the Aermet core for an operating temperature of 100 °C

Appendix B:

PHASE DIAGRAMS OF NI-FE, CU-NI, AND CU-FE

The following page shows the binary phase diagrams for the pertinent pairs of metals involved in the system to be diffusion bonded.

The topmost diagram, Copper-Iron, is given to demonstrate why diffusion bonding Cu to Fe would be difficult. At 900 °C, a representative diffusion bonding temperature, the solubility of Cu in Fe is only about 1.5%, and the solubility of Fe in Cu is less than 1%. At no temperature below the melting temperature of copper is the solubility of either metal in the other higher than 8.2%.

The middle diagram, Copper-Nickel, shows that the two metals are entirely miscible in one another at any composition.

The bottom diagram, Iron-Nickel, shows that above 912 °C, Ni and Fe are completely miscible in one another. It also shows that at lower temperatures and different compositions, various intermetallic compounds are formed. Whether these will be formed during diffusion bonding, and whether they will have an effect on the bond, remains to be determined by further experiment.
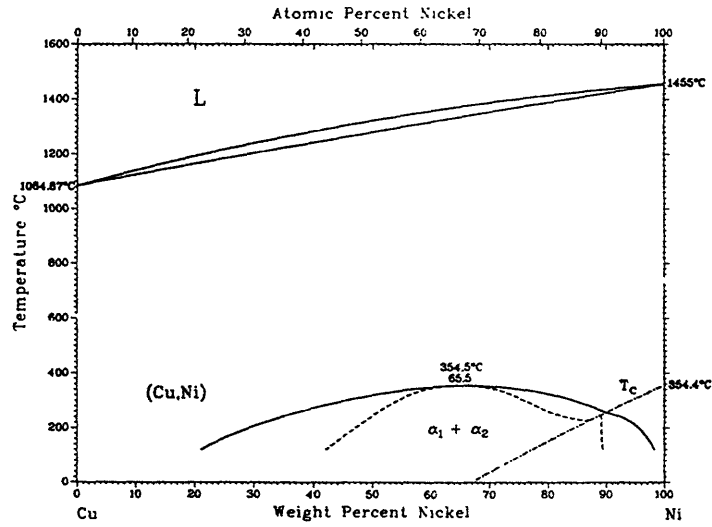
Source:

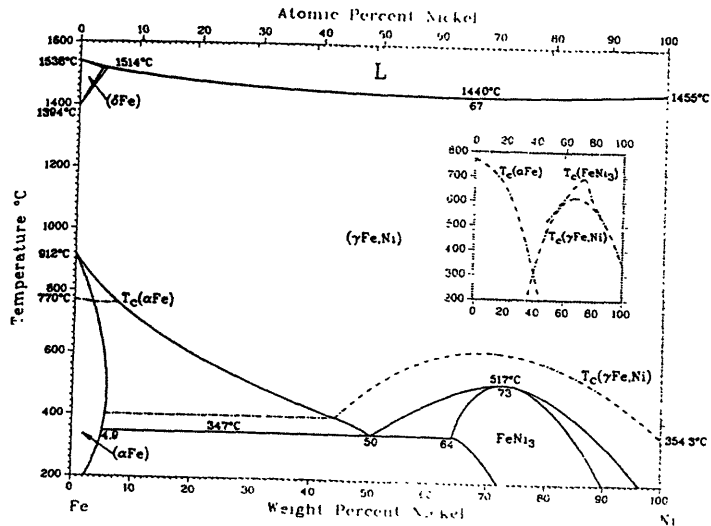ASM Handbook, Vol 3: Alloy Phase Diagrams. (1995). Materials Park, OH: ASM
    International.

Cu-Fe

Cu-Ni

Fe-Ni

110
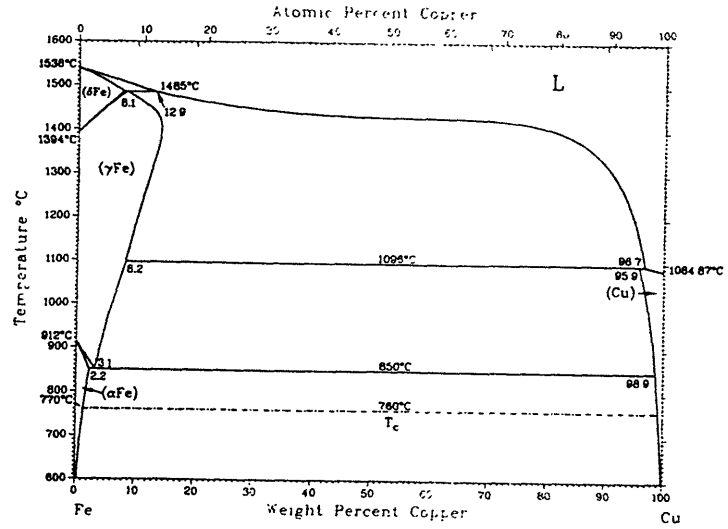
Appendix C:

VENDOR QUOTATIONS

The cost of the new, open slot core, diffusion bonding process presented in this thesis was determined by a combination of vendor quotations and calculations of machining and assembly times. The vendor quotations were obtained for the parts by using modified drawings of the starter/generator geometry.

There are two quotations from the investment casting house, Hitchiner Manufacturing Company, Milford, NH. These are for the open slot, Aermet 100 magnetic core and the 410 stainless steel impellers. The geometries of both these parts are in the text. Note that the quotation for the impeller castings includes material cost, while the quotation for the core does not. This is due to the fact that Hitchiner does not ordinarily cast Aermet, and would have to do so for this job. One reason the Aermet core is so much more expensive than the impellers is because the Aermet must be vacuum cast, while the stainless steel does not.

The quotation for the bars and end rings is from the Cadi Company, Naugatuck, CT, a supplier of copper and copper alloy products. Note that the price depends on the current price for copper.

The diffusion bonding process is not currently performed industrially, so the nearest conservative approximation is given. This is for the bonding of copper and Aermet in a HIP unit using a cycle that has been standardized to densify titanium castings. The quotation includes some experimentation and an estimate for work done in quantity. The quotation is from Industrial Metals Technology (IMT) Inc., Andover, MA.

HITCHINER
MANUFACTURING CO., INC.
MILFORD, NEW HAMPSHIRE 03055

ISO-9001

CERTIFICATED FIRM

QUOTATION

Date:	October 6, 1995

SATCON TECHNOLOGY CORP
161 FIRST STREET
CAMBRIDGE MA 02142-1207

Our Ref: 15-0687-01

Your Ref: 950926

Dated: 09/28/95

Attn: CHRIS BROWN

We propose to furnish investment castings at prices and conditions outlined below:

Dwg. No: SK509   Rev: NONE   Part Name: ROTOR STACK STARTER/GEN

TOOLING PRICES
<u>Mold</u>   <u>Fixtures</u>
7000.00

CASTING PRICES

<u>Quantity</u>			<u>Unit Prices</u>		
200	& UP	PC	$ 50.00	Material:	1020
100	& UP	PC	$ 55.00	Heat Treat:	ANNEAL/OVERAGE
50	& UP	PC	$ 60.00	Weld Repair:	YES
				Pickle/Passivate:	NO

<u>Applicable Specifications</u>
General: AERMET 100

NOTE: Part dimensions and other technical criteria not itemized below will be furnished as specified on reverse side hereof or to print tolerances, whichever is greater.

THE ABOVE COST IS FOR YOUR COST EVALUATION ONLY AT THIS TIME AND IS BASED ON THE ALLOY (AERMET 100) BEING SUPPLIED BY YOU. SINCE THIS IS A NEW ALLOY WHICH MUST BE POURED IN A VACUUM, IT WILL BE NECESSARY FOR US TO RUN SAMPLE HEATS TO PROVE OUT OUR PARAMETERS AND PROVE THE CASTABILITY OF THE ALLOY. AT THIS TIME IT IS NOT POSSIBLE FOR US TO GUARANTEE THE MECHANICAL AND PHYSICAL PROPERTIES THAT ARE SPECIFIED ON THE CARPENTER SPEC SHEET. WE WILL RUN TENSILE TESTS ON SEPARATELY CAST TEST BARS. ANY ADDITIONAL TESTING WOULD HAVE TO BE MUTUALLY AGREED UPON PRIOR TO INITIAL ORDER.
WE WILL REQUIRE FINALIZED FULLY DIMENSIONED CASTING DRAWINGS.
OUR SHIP TOLERANCE IS PLUS OR MINUS TEN PERCENT. OUR TERMS ARE ONE PERCENT 10 DAYS, NET 30 DAYS FROM DATE OF INVOICE. PARTS WILL SHIP F.O.B. MILFORD OR LITTLETON, NH.

DELIVERY
SAMPLES: We propose to furnish 1 sample 11 weeks after receipt of order.
PRODUCTION: The first delivery will be 9 weeks after sample approval.

This offer subject to terms and conditions on reverse side hereof.

THANK YOU FOR THE OPPORTUNITY TO OFFER YOU OUR QUOTATION.

HITCHINER MANUFACTURING COMPANY, INC.

FRITZ MARSTON
N.B. SALES ENGINEER

HITCHINER
MANUFACTURING CO., INC.
MILFORD, NEW HAMPSHIRE 03055

ISO-9001
DNV
CERTIFICATED FIRM

QUOTATION

Date:	October 6, 1995

SATCON TECHNOLOGY CORP
161 FIRST STREET
CAMBRIDGE MA 02142-1207

Our Ref: 15-0687-02

Your Ref: 950926

Dated: 09/28/95

Attn: CHRIS BROWN

We propose to furnish investment castings at prices and conditions outlined below:

Dwg. No: 2001047   Rev: NONE   Part Name: IMPELLER ROTOR START/GEN

TOOLING PRICES
<u>Mold</u>   <u>Fixtures</u>
9675.00   S/ARM   1430.00

CASTING PRICES

<u>Quantity</u>			<u>Unit Prices</u>	Material:	410
200 & UP	PC	$	12.00	Heat Treat:	ANNEAL
100 & UP	PC	$	13.00	Weld Repair:	YES
50 & UP	PC	$	14.00	Pickle/Passivate:	NO

<u>Applicable Specifications</u>
General: 410SS

NOTE: Part dimensions and other technical criteria not itemized below will be furnished as specified on reverse side hereof or to print tolerances, whichever is greater.

CASTINGS WILL BE FURNISHED PER THE ATTACHED MARKED PRINT, DATED 10/6/95.
THIS QUOTATION WILL BE SUBJECT TO REVIEW UPON RECEIPT OF YOUR FINALIZED,FULLY DIMENSIONED CASTING DRAWINGS.
OUR SHIP TOLERANCE IS PLUS OR MINUS TEN PERCENT. OUR TERMS ARE ONE PERCENT 10 DAYS, NET 30 DAYS FROM DATE OF INVOICE. PARTS WILL SHIP F.O.B. MILFORD OR LITTLETON, NH.
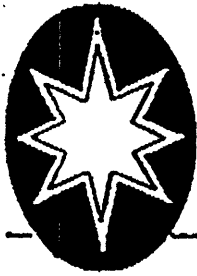
DELIVERY
SAMPLES: We propose to furnish 1 sample 13 weeks after receipt of order.
PRODUCTION: The first delivery will be 9 weeks after sample approval.

This offer subject to terms and conditions on reverse side hereof.

THANK YOU FOR THE OPPORTUNITY TO OFFER YOU OUR QUOTATION.

HITCHINER MANUFACTURING COMPANY, INC.

FRITZ MARSTON
N.B. SALES ENGINEER

Cadi Company Inc.
RESISTANCE
WELDING PRODUCTS

FAX TRANSMITTAL SHEET

To: **SATCON**

Date: 10-2-95

Fax No.: 617-661-3373

No. of Pages: 1

Attention: **Chris Brown**   From: Rocco Sr.

Message: We are pleased to quote as follows:

5000 ft. Alloy 182, Chromium Copper

Hot Extruded per B/P SK 510 (No Heat Treat)

Approx 2300# @ 3.97 #

One time tooling charge $2850.00

50 ft. Alloy 182, Chromium Copper Tubing

3" OD x 1 1/2" ID Hot Extruded (No Heat Treat)

Approx. 1025# @ 3.89#

Delivery: Item #1 10/12 weeks
                "   2   7 weeks

FOB: Naugatuck CT

Prices based on Comex Copper @ 1.30#

Regards,

Rocco

 Densification • P/M Products • Composite Materials

. 20, 1995

 is Brown
 n Technology Corp.
 st Street
 dge, MA 02142-1221

 17-661-3373
 JECT: Bonding of Induction Rotor Components

 aris,

 reference to the above subject and your correspondence with John Hebeisen and
 ck, IMT submits the following quotation:

 totype:

 otation is based upon the assumption that Satcon will supply all the rotor
 ents including the impeller caps.

 ll fabricate an 18ga (.049") low carbon steel sleeve to complete the capsule. We
 an and assemble the rotor components, weld the fabricated sleeve to the caps and
 shaft to the Impeller caps on each end of the assembly. An evacuation stem will
 ed to the O.D. of the steel sleeve. Once the welding of this assembly is complete
 helium leak check, hot off gas (600F) and seal under vacuum.

 nding of the prototype assembly will take place in (1) 8" HIP cycle.
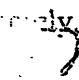
 al price for the above described work will be $2105.00.

 M. Production Pricing:

 M. pricing for approx. 1000 pieces with dimensions of approx. 3" dia. x 10"
 ll be $105.00 each.

 ice includes the assembly, welding, leak checking, offgassing, sealing and HIP.

 yment terms are net 30 days. Delivery of the prototype piece will be 3-5 weeks
 ceipt of order and components.

 nk you for this request. Please call on us if we can be of further assistance.

 ely,

 cGinnis
 anager

115